2015-01-01

Multi-3D System: Advanced manufacturing through the implementation of material handling robotics

Jose Luis Coronel Jr.
University of Texas at El Paso, jlcoronel@miners.utep.edu

MULTI^{3D} SYSTEM: ADVANCED MANUFACTURING THROUGH THE IMPLEMENTATION OF MATERIAL HANDLING ROBOTICS

JOSE LUIS CORONEL JR.

Department of Mechanical Engineering

APPROVED:

Ryan B. Wicker, Ph.D., Chair

David A. Roberson, Ph.D.

Yirong Lin, Ph.D.

Charles Ambler, Ph.D.
Dean of the Graduate School

Dedication

This Thesis is Dedicated To My Grandmother, Benita Lugo, Who Led Me to the Lord, as well as To My Parents and Family, Who Immensely Supported My Academic Pursuits.

MULTI^{3D} SYSTEM: ADVANCED MANUFACTURING THROUGH THE IMPLEMENTATION OF MATERIAL HANDLING ROBOTICS

by

JOSE LUIS CORONEL JR., B.Sc. in Mechanical Engineering

THESIS

Presented to the Faculty of the Graduate School of

The University of Texas at El Paso

in Partial Fulfillment

of the Requirements

for the Degree of

MASTER OF SCIENCE

Department of Mechanical Engineering

THE UNIVERSITY OF TEXAS AT EL PASO

December 2015

Acknowledgements

I would firstly like to acknowledge Dr. Ryan Wicker, director of the W.M. Keck Center for 3D Innovation (Keck Center), for his support in all of the research I conducted throughout my graduate studies. Mr. David Espalin, manager of the Keck Center, receives my sincerest gratitude for his constant guidance and mentorship. Together, these two individuals provided for me an environment for discovery, challenges, and rewarding successes. I will always be grateful to Dr. Ryan Wicker and David Espalin for their involvement in my academic pursuits. The efforts of my committee members should also be acknowledged, therefore I thank Dr. Yirong Lin and Dr. David A. Roberson for their support on reviewing my work and taking part in a very meaningful accomplishment in my life.

Additionally, I would like to acknowledge America Makes, the National Additive Manufacturing Innovation Institute, which funded this project. America Makes is funded by the Office of the Secretary of Defense, Manufacturing and Industrial Base Policy, Manufacturing Technology, through a cooperative agreement with the Air Force Research Laboratory (FA8650-12-2-7230). I would also like to acknowledge Northrop Grumman, rp+m, Lockheed Martin, the University of New Mexico and Youngstown State University for their contributions in this project. I would also like to thank Stratasys, specifically Mr. Bob Zinniel for his technical support during the mechanical modifications of the FDM machines and providing an understanding of the FDM process and Mr. Ron Schloesser for his technical support that enabled communication and control of the FDM machines.

A great deal of Keck Center staff members supplied valuable input in the presented research, and should be acknowledged. Mr. Steven Ambriz, provided an inspired design for the components that were transferred by the robot. Ms. Alexandra Alcantara-Guardado had much input in the logic behind the programming architecture. I acknowledge the following people: Dr. Chiyen Kim, Mr. Alfonso Fernandez, Mr. Alejandro Cuaron, Mr. Jorge Ramirez, and Ms. Graciela Bribiescas for their assistance in multiple facets of the research. I additionally would like to thank

Dr. Benjamin Flores, Mrs. Ariana Arciero-Pino, and Mrs. Sara Rodriguez of the Louis Stokes Alliance for Minority Participation (LSAMP) program at the University of Texas at El Paso, for their support through the National Science Foundation's Bridge to the Doctorate Fellowship (NSF grant number HRD-1301858).

I would like to conclude with the acknowledgment of those who have supported me outside of the academic setting, my family. My parents, Jose Luis Coronel and Evangelina Coronel, my sister Jasmin, and my brother Edward whom always encouraged my affinity for academia. I thank God, for the health, strength and focus I needed to get through graduate school. Finally, I greatly thank the congregation of Templo Emmanuel, for their prayers, and for encouraging me as I stepped into the world of higher education.

Abstract

Since the rise of additive manufacturing (AM), innovation has been at the forefront. Additive Manufacturing systems that incorporate complex processes are steadily being developed. One example is the Multi^{3D} System, which was designed to integrate the ability to print multi-material parts with that of embedding electronics. To achieve this automated process, the Multi^{3D} incorporates a six-axis robotic arm to transfer a build platform containing a printed part, to various manufacturing stations (two fused deposition modeling (Stratasys, FDM400mc) systems and a computer numerical control router (Techno CNC Router). The robot is a Yaskawa Motoman MH50 chosen for its payload capacity of 50 kg. This research focused on the analysis of motion to determine the placement of the components (manufacturing stations) of the Multi^{3D} System. One fused deposition modeling station was completely modified and tests were made to determine the validity of the modified system, compared to an unmodified 3D printer. There were several factors considered for the positioning of the components, including the reach of the robot, the addition of future components, and the design space. These were validated after developing simulations through CAD (Computer Aided Design) modeling, along with theoretical calculations using Denavit-Hartenberg matrices. Testing of the system proved placement of each manufacturing station to be at a specified distance of 1.47 m.

LabVIEW programming was possible through ImagingLab's Yaskawa robot library. The programming architecture was made to allow certain functions, such as the menu and the pause function. The Menu allows the user to determine the order in which the platform will be transferred, while the Pause function allows the user to interrupt the process for inspection or corrections to be made. The programming also allowed the incorporation of various sensors and acutators, making possible the limited human interaction that was key to the Multi^{3D} System. With limited user input, it is possible for the process to be repeatable, accurate and operational for long periods of time. Through programming, the robot was able to be successfully utilized for a variety of experiments.

The robot was used to test multiple traveling objects – the portable build platform and the traveling envelope. From these tests some modifications were recommended to facilitate the placement of the platform and envelope, improving the placement accuracy. Alignment bars and brackets showed improved repeatability in component placement. After modifications, a test was conducted to print a stair step with and without a pause. The pause function for the modified FDM consisted of pausing the build, placing the envelope on the platform, and removing the entire assembly. The reverse was done to allow for printing to resume. After completed, the stair step was compared to one created by the unmodified 3D printer. Results showed the tolerance for both systems in analyzing the layer offset is well within +51μm (0.0020") and -25μm (0.0010") from a centerline. This test served to validate that the modified machine printed with results comparable to the original Fortus 400mc machines, but more importantly, it confirmed that the removable platform can be placed and removed accurately by the robot. This is paramount to ensure that the addition of the second modified 3D printer will not have a significant effect on accuracy, and therefore, multi-material parts will possibly be built in the future.

Table of Contents

List of Tables

List of Figures

Chapter 1

Introduction

1.1 Background

Most commonly referred to as 3D printing, Additive Manufacturing (AM) is the process in which an object is built through a process of layer-by-layer deposition of material. (Berman, 2012). This is possible through the use of computer-aided design (CAD) models. By obtaining parts from CAD software, AM allows for the construction of complex geometries (Sun, Rizvi, Bellehumeur, & Gu, 2008). Aside from the ability to produce parts not common to traditional manufacturing methods, AM also reduces the amount of tooling necessary, when compared with conventional manufacturing processes. The applications of this technology are abundant. As of now, AM can be found in the construction of aerospace parts, electronics, and even in the medical field by customization of dental products and hearing aids (Mellor, Hao, & Zhang, 2014).

Although there are various technologies used for AM including the use of metals, polymers and liquid resins, the focus of this work is on the technology known as Fused Deposition Modeling (FDM). This method of 3D printing functions through the softening of polymers into a flowable state. This semi-liquid is then deposited by a nozzle to form a cross sectional slice of the part being printed. The layer of polymer self-hardens, and the subsequent layer can be deposited (Sun, Rizvi, Bellehumeur, & Gu, 2008). The steps are repeated until the final result is a physical part of a CAD model. The world of AM has been expanding throughout these last few years, to the point that it has begun to intersect with other technologies, such as robotics.

Robotics has developed a cooperative relationship with AM. One area of research has delved in the fabrication of printed robotic systems. Here, methods are developed to 3D print components to be assembled with electronics, or preassembled components for robotic implementation. For example, the creation of a 3D printed robotic hand through the individual printing and assembly of fingers with four degrees-of-freedom (Mavroidis, DeLaurentis, Won, & Alam, 2000). Although the printing of robotic components is important to those in the AM

community, the purpose of this document is to divulge the relationship between the two entities that are 3D printing and robotics, in different roles. In this area of research, robotics are programmed to aid in the manufacturing of 3D printed parts.

A major reason for AM to be utilized with other technologies, is that printed parts have limited functionality. Work done by the W.M. Keck Center for 3D Innovation at the University of Texas at El Paso, highlights the possibilities of multi-functionality in 3D printed parts (Espalin, Ramirez, Medina, & Wicker, 2012). Testing of printed parts has proven that they are limited in their mechanical strength. Research has been conducted in adding wires that can improve strength. In order to add the wire reinforcements, requires the printed parts to interact with a manufacturing station, such as a CNC router, that can machine paths for the wires. This however, cannot be completed in a way that will allow a multi-functional part to be printed partially, embed wires, and resume printing to encapsulate them. In order to create truly multi-functional parts, it is necessary to interrupt the printing process at a predetermined layer, so that components can be embedded. This becomes a tedious process for an operator to complete, thus enters the need of a material handler. A robotic material handler would allow the transfer of the printed part around the stations needed, in order to encapsulate the components desired in a print. A robot can execute operations quickly, accurately and with high repeatability that would take the burden off of the user.

1.2 Motivation

Engineers and scientists are often left to contemplate what the next step is, when encountering a breakthrough in their research. The field of AM is no exception. 3D printing has a plethora of applications; which companies have identified as advantageous in their desire to create quick models of their product. However, as stated earlier, the inquisitive mind is always interested in where the technology is heading. The Multi^{3D} System, a project funded by America Makes, an initiative by President Obama aimed at advancing the development of additive manufacturing, aims directly at answering the question of what is next for 3D printing.

The Multi^{3D} System is the complete integration of multiple manufacturing technologies. This includes two FDM machines, most commonly referred to as 3D printers, among other technologies to be discussed later in the document. It is most common for FDM machines to work individually in printing a desired CAD model. Using one 3D printer is not a great limiting factor, as there have been several advancements made within one FDM. Printed electronics with conductive inks and a 3D printed motor are both the result of experimentation with one FDM. This research was also performed by the W.M. Keck Center. However, the use of two FDM machines allows the utilization of multiple model material from which to print with. This would lead to multi-material printing. Other possibilities arise with multiple printers working in synchronization. Different depositions strategies can be used. One machine would have a large extrusion tip for printing thicker layers, while the other could print thin layers with a small printing tip. Another benefit of multiple printers is the introduction of parallel manufacturing. Parts could be printing simultaneously on each of the printers, and each could be taken to be machined at separate times. Putting aside singularity, the purpose of the Multi^{3D} System is to amalgamate current technologies to create a system that will make possible the printing of electronic devices in a one-stop manufacturing location.

What encompasses the motivation behind the research conducted through this project is the following. Incorporating multiple manufacturing stations will allow for multi-material parts to be printed, as well as make possible the machining of the parts for insertion of electronic components. The results of this research will be the possibility to print satellites that are ready for operation as soon as they are removed from the 3D printer. There are other future applications that would arise through the success of the Multi^{3D} System, and some of the accomplishments made and the future work will be discussed in this thesis.

1.3 Thesis Objectives

The objectives this thesis will address throughout include the following:

1. Determine the placement of the components (i.e. manufacturing stations) of the Multi^{3D} System.
2. Develop a program that will define the robotic motions required for execution of the Multi^{3D} System.
3. Experimentally validate component placement and system programming.
4. Discuss results of printed parts created by the Multi^{3D} System

1.4 Thesis Outline

The structure of this thesis is such that it will give the reader an understanding of what is being accomplished through the creation of the Multi^{3D} System. Chapter 2 will contain a literature review referring to journal papers that provided a basis to the final product of this project. This includes a study of what has been accomplished with robotics, as well as the benefits leading to their implementation. Although robotics are most common to industrial settings, some of the methodologies created in how they interact with objects will be used as guidelines for incorporating them to AM. In chapter 3, the discussion will focus on the parameters that determined the finalization of component placement for the system. Chapter 4 will present the programming architecture. Here, some of the characteristics of robot systems are implemented, such as safety precautions, found in industrial applications. The methodology for transferring parts within the system will also be discussed in the fourth chapter. This is followed by a results section in chapter 5, where the various tests conducted with the robot are discussed. Included are some of the design changes that were brought about to various components of the system due to their interaction with the robot. Finally, the conclusion will highlight the findings of the research and present the future work planned including design changes and further experimentation with the Multi^{3D} System.

Chapter 2

Literature Review

2.1 Introduction

The focus of the conducted research was on the application of robotics in manufacturing systems, and the benefits of applying robotics to the ever expanding world of AM. The inclusion of robotics in the Multi^{3D} System involved a study of kinematics, as well as a general review of the technology proposed. This included validations to the utilization of robotics for the system as demonstrated in previous scientific work.

2.2 Implementing Robotics

As robotics technology has matured, robots have been implemented in a myriad of applications throughout the world of manufacturing. The automobile industry is one of the most recognizable consumers of robotics, as it utilizes large robotic systems to help assemble vehicles rapidly and efficiently. The function of robots within this industrial setting include assembly of the car body, applying paint and coatings on various parts, press tending, and the partial assembly of the engine and power train (Brogårdh, 2007). Since the automotive industry is the largest customer of industrial robots, much of the development to robots is being guided by the demands of the automotive industry. These demands include the implementation of robots in the final assembly of vehicles, when the tasks are complex and there is variation in the geometries of the products (Brogårdh, 2007). Although the technology is not yet at the point where robots are intuitive, any system that requires repetitiveness in the transferring of an item from one position to another, would likely benefit from the use of robotics. As additive manufacturing progresses into the creation of large scale, multi-functional parts, the possibility of incorporating robotics emerges. In the present work, research was conducted to identify the manner in which robotics should be employed and the reasoning behind its selection. One major benefit of utilizing robots is that you acquire the ability to effectively coordinate the transfer of objects throughout a system (Doren & Slocum, 1995).

Implementation of robotics in a system varies. One example is the research conducted by Doren and Slocum (1995) on the robotic transfer of silicon wafers for fabricating semiconductors. Doren and Slocum highlight some of the most prominent benefits of utilizing robotics. The primary benefit is found in eliminating the need of a human worker to physically move cassettes of wafers. This decreases particle generation, which is important for removing contaminants in parts that require a clean environment. The second benefit mentioned is the fluid motion that robotics provides, mitigating the vibration of objects that could possibly damage the product. Another beneficial aspect of integrating robotics into a system, is the inherent repeatability and accuracy brought forth by programmable commands (Doren & Slocum, 1995).

The use of robotics is ideal for the Multi^{3D} System considering that printed parts need to be accurately transferred between the various manufacturing stations. After the review of current publications related to AM and robotics, a gap was identified in the use of robotics with AM technologies. The need to identify the proper robot for the Multi^{3D} System led to a study of the categories of robots. There are three main types of industrial robots as identified by Ravi, J. These types are: 1) Assembly Robots, 2) Robots as tool handlers, and 3) Material handling robots (Ravi, Murugesh, Srivatsa, Sastry, & Raman, 1988). The Yaskawa Motoman MH50 that was utilized for the research conducted, is multi-purpose and could have been utilized for any of the three applications mentioned. However, in regards to the Multi^{3D} System, the MH50 fell under the material handling category. An application of material handling robotics is found in MITPICK – a robot that was designed specifically for unloading casting from a die casting machine (Ravi, Murugesh, Srivatsa, Sastry, & Raman, 1988). Ravi *et al.* mentions the use of selecting programming or the robot specific for its application. Yaskawa, the company from which the MH50 robot was purchased, provided a robot library that greatly simplified the operation of the robot through the use of LabVIEW (the programming interface used in the present work). However, positioning the robot in the desired location at any time was not the bearer of complexity. Utilizing robotics in a system brings forth safety concerns that must be addressed in the overall programming. The researchers of the MITPICK mention that if the system stopped because of

some error, the machine cannot resume without awareness of the operator. These safety precautions are precedents to what was implemented in the Multi^{3D} System, and will be discussed further in Chapter 4. They are referred to as safety circuits, as they consist of loops that oversee the readiness of various components of the system.

The approach to moving objects around an assembly type setting has varied depending on the type of object and the manipulator. A flexible manufacturing system was studied, involving the use of distributive control design (Spathopoulos & de Ridder, 1999). It utilizes subsystems that control inputs and outputs, much like the Multi^{3D} System used, as explained in Chapter 4. The study conducted by Spathopoulos *et al*., included the use of conveyer belts, CNC lathes, storage areas, and robot manipulators. The implementation of distributive control, consists of establishing the control objectives, then having the controller designed to complete the stated objectives (Spathopoulos & de Ridder, 1999). A similar approach is taken for the Multi^{3D} System, as will be presented in a later section, where the DX100 controller is explained, including its role in the system, and the method in which it incorporated inputs and outputs, similar to the flexible manufacturing system. The use of the Yaskawa MH50 greatly simplified the control of the manufacturing system, because there is only one, and the objects it interacted with were only the portable build platform and the travel envelope. This means that there was no variation to the object handled, reducing the risk of error. Next, a methodology of transferring these objects will be contemplated.

Research conducted by Sayler and Dillmann (2011) identifies the need to have a simulated system before the full implementation of a robotic operated system, and the use of a human operator to give instructions while the system develops. Sayler *et al.* identify eight subtasks that are implemented in the transfer of an object from one point to the other. These tasks are listed as 1) transfer to object 2) approach object 3) pick object 4) depart with object 5) transfer to destination 6) approach destination (place object) 7) release object 8) depart from assembly (Sayler & Dillman, 2011). The methodology in placement and removal of objects is directly compatible with the Multi^{3D} System in the manner in which the robot would transfer the portable build platform and

the heated travelling envelope. Problems arise when encountering errors in the location of the object. This displacement can lead to object loss, or collision of the object with the robot grippers (Sayler & Dillman, 2011).

The use of robotics in a system has been discussed as a means to provide efficient repeatable transport of parts. The robots of interest, one of which will be utilized in the Multi^{3D} System, are defined as material handling robots. Safety precautions are essential for any robot use. The nature of a programmable robot is, that if something goes wrong but the robot has no signal to recognize the error, the process will continue and collisions might occur. For this reason safety circuits are used; to ensure the proper use of the system and the safety of any personnel handling equipment around the system enclosure.

Chapter 3

Component Placement

The initialization of the project involved the consideration of various alternatives for the placement of every manufacturing station around a material handling robot. Most of the constraints were based on the size of the part that would be printed by the Multi^{3D} System. Consideration of several build parameters led to the selection of the (Yaskawa Motoman MH50 Robot), as the means of transferring the part from station to station (Motoman, Yaskawa Motoman Robotics, 2012). Aside from the ideal size of printed parts, other build parameters included the size and weight of the platform upon which the part would be printed, the workspace available, and the manufacturing stations it would interact with. The MH50 met the specifications and as an extra incentive, a robot library for LabVIEW had been recently released. With LabVIEW expertise in-house, communication would be facilitated. The payload of the MH50 robot is 50 kg (110.3 lbs), appropriate for its planned application within the Multi^{3D} System. The payload was important for the design of the portable components that would interact with the robot, taking into consideration the maximum weight allowed. This chapter will discuss the reasoning behind the location of each manufacturing station of the system around the robot, including some robotic control theory overview, and simulations conducted prior to the installation of each station.

3.1 Denavit-Hartenberg Parameters

The position and orientation of a robot can be determined through key parameters. These are, the lengths of the links and the angles of rotations. Being a six axis robot, there are six links and angles that must be identified in order to know the position of the robot. The Denavit-Hartenberg (DH) parameters, developed by Jacques Denavit and Richard S. Hartenberg, provide an approach for calculating the location of the robot (Denavit & Hartenberg, 1955). There are two types of motion of the links that are accounted for in the Denavit-Hartenberg convention. One is rotation along its centerline, or base rotation as shown in Figure (3.1a). The other is pivoting at a

a)

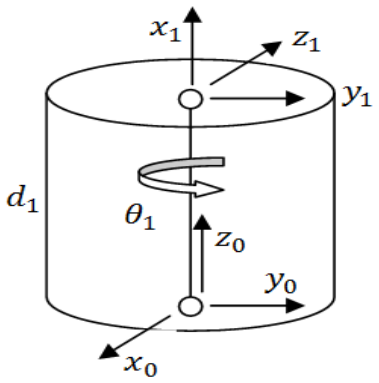

b)

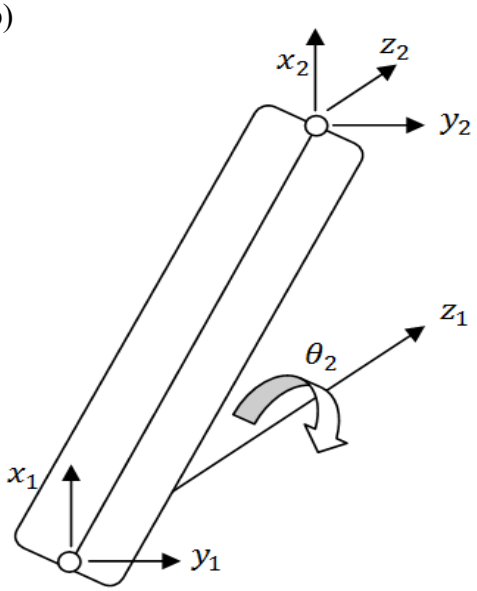

Figure 3.1. Schematic of links. a) Rotating link b) Pivoting link

fixed vertex, Figure (3.1b). The six-axis robot utilizes both these types of motions, to perform any specified task. The bottommost point of each link in Figure 3.1 is the origin, and the topmost point is the coordinate system of the subsequent link. The coordinate system shift from the initial point to the end point can be described by the A-matrix (Lewis, 2004). The A-matrix is found on Figure 3.2, where the i, corresponds to the link number that the matrix is being applied to. The variable a_i represents the length of link i, and d_i is the distance between the origin and final point when a link rotates along the center axis, Figure (3.1a). The final variable α_i, identifies the twist in link i, but for simplification purposes we assume the links to be rigid, as the robot links are not easily twisted (Lewis, 2004).

$$A_i = \begin{bmatrix} \cos\theta_i & -\cos\alpha_i \sin\theta_i & \sin\alpha_i \sin\theta_i & a_i \cos\theta_i \\ \sin\theta_i & \cos\alpha_i \cos\theta_i & -\sin\alpha_i \cos\theta_i & a_i \sin\theta_i \\ 0 & \sin\alpha_i & \cos\alpha_i & d_i \\ 0 & 0 & 0 & 1 \end{bmatrix}$$

Figure 3.2. A-matrix of any given link, *i* of the robot

When implementing the DH parameters, the convention calls for any rotation or pivoting motion to be along the z-axis. This convention allows for the compilation of multiple matrices to assemble what is called the T-matrix. Through the T-matrix, it is possible to determine the position

and orientation of the robot in relation to the base. Figure 3.3 shows the equation of how the T-matrix is compiled. It involves the multiplication of all the matrices, and results in a three by three coordinates that show the rotation and a column (Lewis, 2004).

$$T_i = A_1 A_2 \dots A_i = \begin{bmatrix} R & P \\ 0 & 1 \end{bmatrix}$$

Figure 3.3. T-matrix using DH parameters

The DH parameters were obtained from the CAD model of the Yaskawa Motoman MH50 provided by Yaskawa. Lengths of each link were taken from the CAD and can be seen on Table 3.1. These values were utilized in order to obtain the T-Matrix. MATLAB programming was implemented in order to make matrix calculations simpler. Through the values found in the table and the equation on Figure 3.2., the A-matrix was calculated for each of the robot's links. Figure 3.4. shows where each of the links can be found on the robot, as well as a schematic of how each coordinate frame was positioned in order to calculate the matrices. The A-matrix accurately represents the three dimensional distance of any link to the origin, as well as the orientation of the end point. When all six A-matrices are compiled, the T-matrix can be generated. These matrices can be found in Appendix A throughout the MATLAB code. Multiplying the matrices together, it is possible to determine the position of the center of any of the robots' axes in relation to the base.

Table 3.1. Data from the addition of pins to the grippers

Robot Link	Length α*i*	*Distance di*
S	198.8 mm (7.83")	228 mm (8.98")
L	870 mm (34.25")	7 mm (0.28")
U	384 mm (15.12")	143 mm (5.63")
R	37 mm (1.46")	703.5 mm (27.70")
B	163.5 mm (6.44")	33 mm (1.30")
T	0 mm (0")	11.5 mm (0.45")

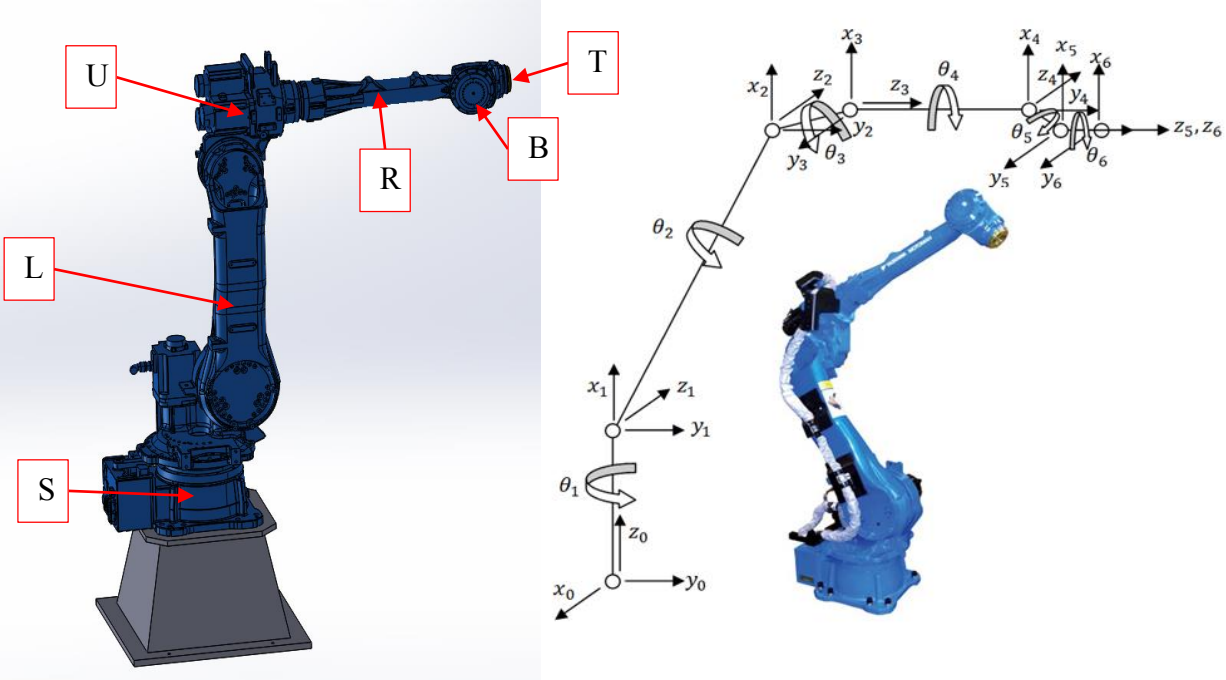

Figure 3.4. Robot Links and DH parameters as applied to the MH50 (Motoman, Yaskawa Motoman Robotics, 2012)

The matrices were utilized to make simulations of where the manufacturing stations should be placed, and make a judgement on whether the positioning of the robot would maximize the use of the available space. Through the DH parameter calculations, Figure 3.5. was created to show the exact position of the robot in two different scenarios. The top image (1) shows the position

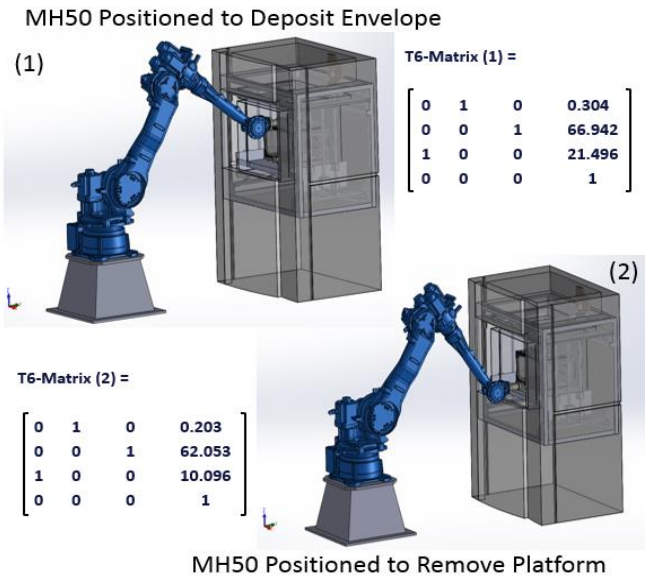

Figure 3.5. Calculated Position of Robot

when the robot is placing the heated travel envelope over the build platform. The T-matrix shows the orientation and the position with respect to the base in inches. The bottom image (2) shows the position where the robot lifts the entire assembly by gripping the build platform. The distance between the stations and the robot were varied until the final positions were determined. Using a list of acquired positions, allowed for the 3D plotting of motion through a simulation of the robot's path. The next section will methodology behind the 3D plots.

3.3 3D Plots

After acquiring the T-Matrix of the MH50, the MATLAB results were compared to a SolidWorks CAD model of the entire setup. The preliminary positions of the FDM machines were determined after several factors were identified. This includes the range of the robot, the payload, among other factors. They will be discussed in more detail in the Final Component Placement section. The CAD model served as a means to confirm the system would work (i.e., the robot

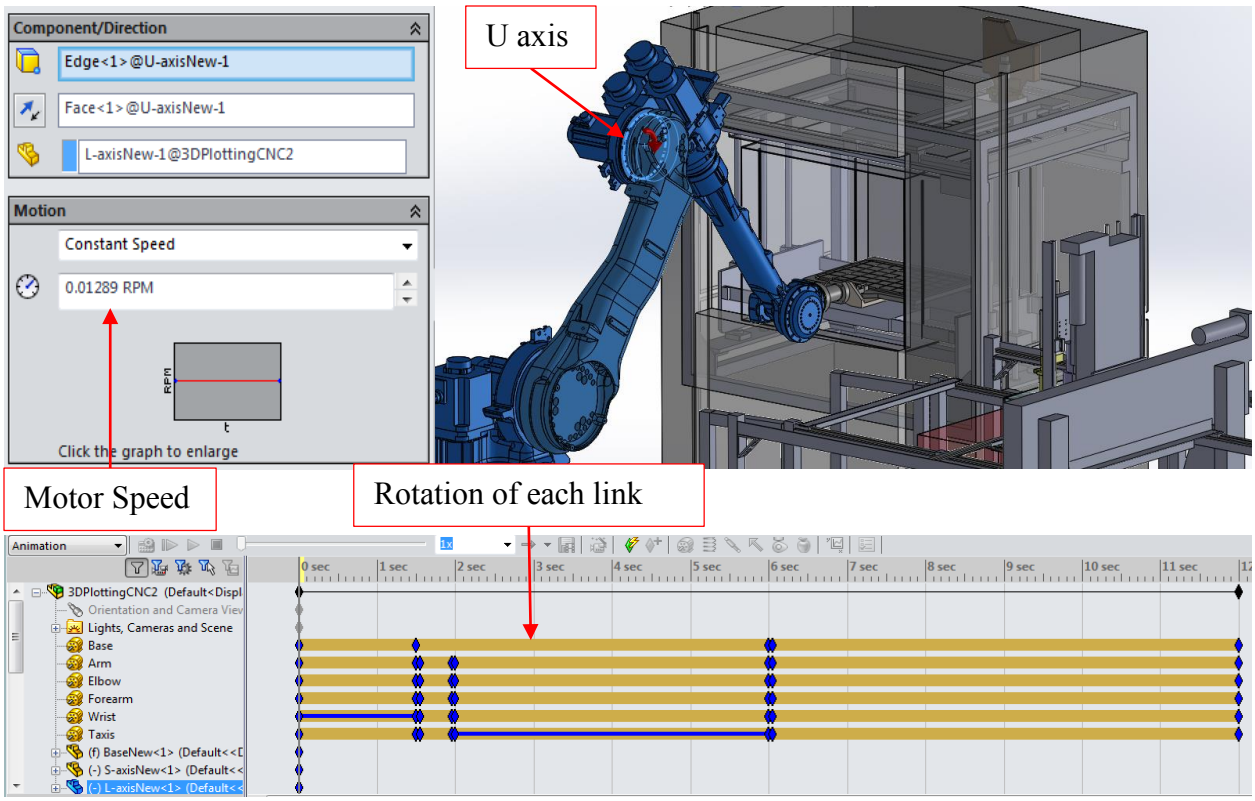

Figure 3.6. Setting RPM for the SolidWorks Motion Study Simulation

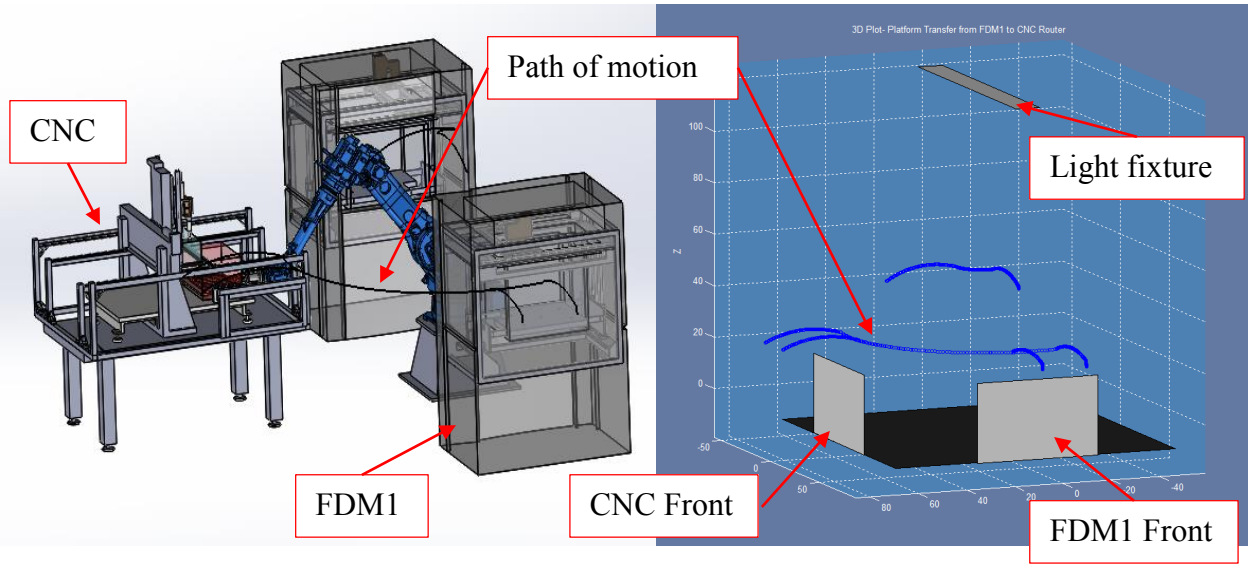

Figure 3.7. 3D Plot of Motion between FDM2 and CNC Router

reaches the interior of each machine and there is clearance to allow the robot's articulation from one machine to another) before the items were purchased. The distance between the manufacturing stations was found and the CAD model was tested through simulations to verify the distance was accurate. During the creation of these motion simulations, neither the robot nor any of the manufacturing stations were present on location, making this study important to determining any collision possibilities beforehand.

The 3D plots were made by using the Motion Study feature in SolidWorks. The positioning desired was conducted by using mating constraints. Next, a servo motor function was created in each of the six links, to allow control of its rotation. The values that were needed were found by finding the change in angle of each link between positions, and converting the distance to a rotational velocity (rotations per minute or rpm). Figure 3.6. shows the input of RPM on the SolidWorks Motion Study on one of the U link of the robot. The simulation took all the rpm inputs and moved the robot accordingly. A simulation was produced to transfer the robot from a position inside one of the FDM machines, to the inside of the CNC. The simulated path can be seen on Figure 3.7., where possible collisions with the walls of the manufacturing stations and the lighting fixtures in the room were addressed. The plot showed the robot had the flexibility to perform the desired task without colliding with any of the surrounding machines. A concern was that when the

robot retracted from the inside a manufacturing station, there would be an elbowing effect, causing a collision with the machine directly behind it. The 3D plotting served to confirm that there would be no collisions during the transfer, and the next step was taken to begin finalizing the positions of each manufacturing station of the Multi^{3D} System. The next section will discuss the reasoning behind the arrangement selected.

3.2 Final Component Placement

The range of the robot, was the primary source of input to the positioning dilemma. According to the specifications provided by Yaskawa, the MH50 has a 2,061 mm (81.1") horizontal reach and a 3,578 mm (140.9") vertical reach (Motoman, Yaskawa Motoman Robotics, 2012). For the purpose of placement, the height limitation was disregarded, and the horizontal reach was taken as the limiting factor since it constrained the distance that components could be placed from the center of the robot. Another large limiting factor to the positioning of the components, was the size of the room and the resources required to power the manufacturing stations. The approximate area that is available for the construction of this Multi^{3D} System is a 5.18 x 7.32 m^2 (17 x 24 ft^2) area without including the power source, the DX100 controller.

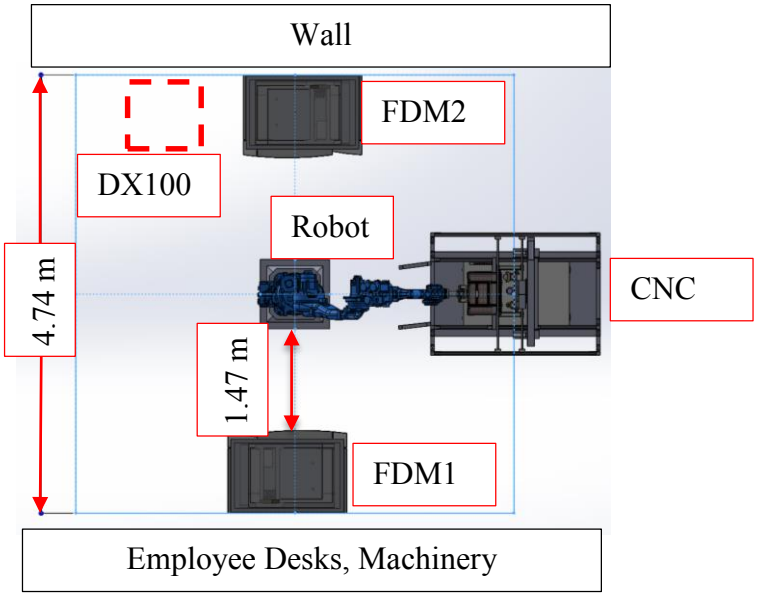

Figure 3.8. Distance between FDM machines

Considering the limited space, the DX100 controller was placed near the upper corner shown in Figure 3.8. Although initially, the plan was to have the controller outside of the specified area, the cabling that powers the robot was not a sufficient length to move the power supply much further. Also, the surrounding area of the build space contains walls, as well as employee workspace which includes tables and other machines. By running through simulations in SolidWorks, it was determined that the most effective positioning of the FDM machines was approximately 1.47 m (58”) from the center of the robot. Figure 3.8. shows the ideal distance between the FDM machines from the furthest point of one to the furthest point of the other. This distance on the CAD model is 4.74m (186.44 in). Although they were theoretical calculations, placement of the manufacturing stations at the predetermined positions has several justifications that will be discussed.

The overall distance between the FDM printers of 4.74 m is well within the design space capacity of 5.18 m in that direction. This confirms the stations can be place in the designated area with no foreseeable conflict. It was noted that the horizontal reach of the robot (2,061 mm) is larger than the selected distance (1,473 mm) between the manufacturing stations and the center of the robot. However, attempting to take full advantage of the robot’s range would result in a completely extended arm. Increasing the distance the robot end effector is from the base will increase the moment caused by the payload. The 941.4 mm (3 ft) pedestal that was purchased for the robot to rest on, was intended to lift the robot to a position where its center of gravity was higher. For the longevity of the robot arm, it requires much less force for the robot to carry the payload near its

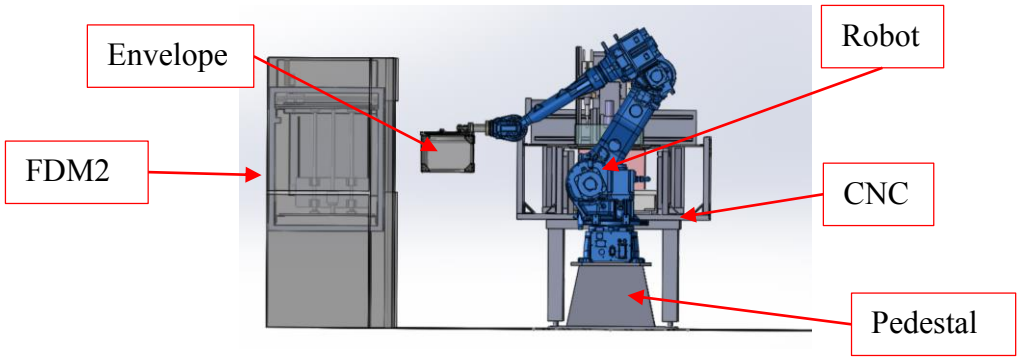

Figure 3.9. Retraction of robot gripping traveling envelope

center of gravity, as opposed to 941.4 mm above. By having the center of gravity closer to the height of the stations where objects would be placed into and removed, there is a reduced risk to damage the servo motors. The chosen horizontal distance is small enough to accommodate the limited working area and the robot's working range, while large enough to allow the robot to retract. Retraction of the robot is limited to a liner movement toward itself. As can be seen in Figure 3.9., retracting the traveling envelope can be completed without the robot's last link moving too closely to the base. At this position it would appear as though the 3D printers could in fact be placed closer than they are, perhaps even reducing the size of the Multi^{3D} System. There are however, some considerations made that would refute that decision.

A simple reason for not having a closer placement of the components, is that there is an increased risk for collisions. The robot being able to retract properly would surely be affected as its end effector would approximate too closely its base. A greater reason for not compressing the Multi^{3D} System is that having the components as far as possible within the workspace, allows for the placement of other manufacturing stations within the system. With the predetermined distance, components can be placed in the gaps between the FDM machines and the CNC router as shown

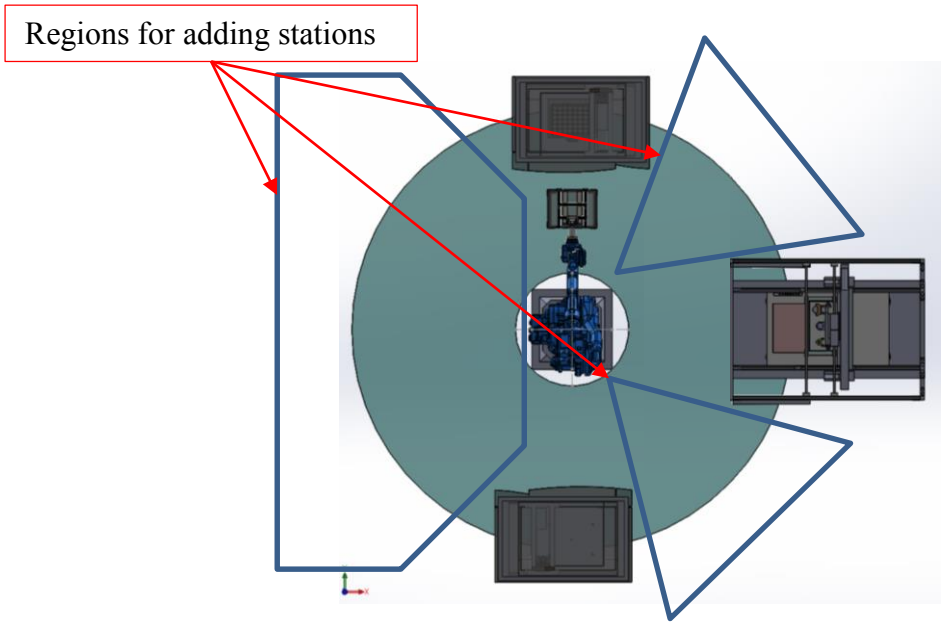

Figure 3.10. Top View highlighting region of possible manufacturing station placement

in Figure 3.10. Other manufacturing stations that could be incorporated include a computer vision camera station for the monitoring of the parts being built. Also, a table for the placement of the travelling envelope when not in use, is another station that would take advantage of the space remaining.

Positioning the CNC router required much of the same considerations as the FDM machines. From acknowledging the distance the robot can reach, the size of the space allocated, and the ability to add more components, the distance of the CNC to the center of the robot should also be approximately 1.47 m. This is the same as the distance between the center of the robot and the FDM machines. Considering the size of the CNC table that was utilized, it would have to be placed on the right side because the workspace is larger in the longitudinal direction, and the CNC would not fit where the FDM machines are placed. Referring to Figure 3.8., the CNC router in place of either one of the 3D printers, would exceed the size of the designated area for the system to reside, protruding into the employee work area. Some considerations made before the arrival of the FDM printers and the CNC router included the actuation of the doors. The Multi^{3D} System aims to limit the human interaction required to manufacture 3D printed parts. Having actuating doors brings forth the concern of possible collision with the robot. The implemented steps to avoid collisions, is to have the door of the 3D printers and of the CNC router, open before the robot approaches anywhere near the desired manufacturing station. Figure 3.11. is an example of a

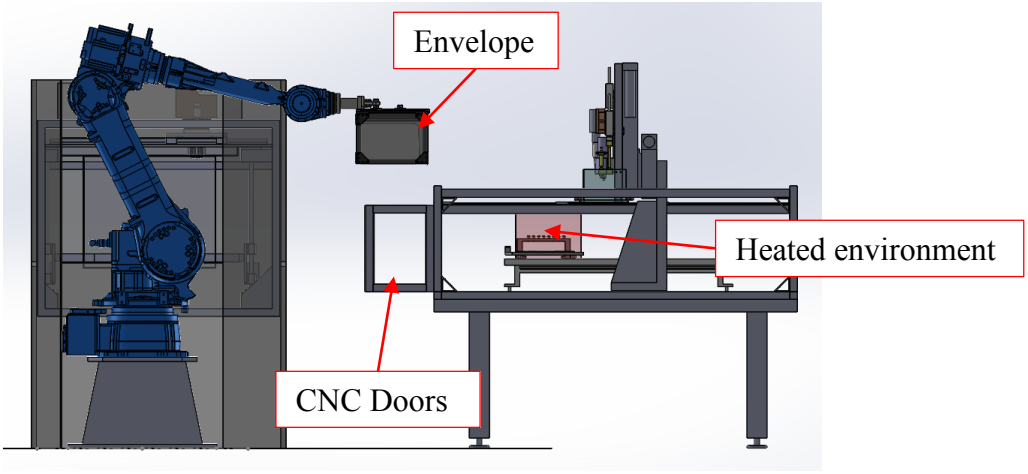

Figure 3.11. Robot avoiding collision with CNC doors

possible approach for entering the CNC router area. It was imperative that the heat loss that will be encountered when moving parts throughout the system was accounted for. A drop in temperature by the 3D printed parts at any time throughout the transfer of the platform could cause warping in the printer part. It was necessary to have the robot near the area of placement, in order to reduce the amount of time the heated regions of the manufacturing stations are exposed to ambient temperature. After obtaining the two 3D printers, and the CNC router, as well as the MH50, experiments were conducted to obtain the validation of the design space. These experiments will be discussed in Chapter 5.

Chapter 4

Programming Architecture

4.1 Description

In order to integrate multiple manufacturing stations, a method of communication was established. The Yaskawa robotics library created by ImagingLab was the means of communication in the synchronization of the project. Not only was the software an enabler for controlling the robot, it allowed the control of multiple devices connected to the DX100 controller. The programming architecture created for the Multi^{3D} System was specifically designed to allow for specific functions and commands to be carried out. These functions include a "Pause" to allow for user interference when necessary, as well as the possibility to assign the order of the processes from initialization. There are also "Menu" functions, as well as safety measures that will be discussed in detail throughout this chapter. Each programming feature required manipulation of loops in the LabVIEW virtual instruments (VI's) to give the desired functionality to the overall program for the Multi^{3D} System.

4.2 DX100 Controller

The motion of the Yaskawa MH50 Robot is attributed to the rotation of the six servo motors, controlled by the DX100. Not only does the DX100 control the MH50, but it is the control center for the myriad of sensors, actuators, and other electronics that comprise the Multi^{3D} System. With its multiple ports, the DX100 has the capability to control 40 inputs and 40 outputs, 16 of each being system inputs/outputs, and the other 24 inputs/outputs being user defined (Motoman, DX100 Robot Controller, 2011). The controller also has eight relay outputs, utilized for when an external power source is powering the electrical component and only a signal is needed. The DX100 operates on 3-phase 240 VAC at 50/60 Hz, and the output voltage for powering electronics is 24V DC with a current capability of 1.5 A. Figure (4.1) shows a diagram of the outputs that are

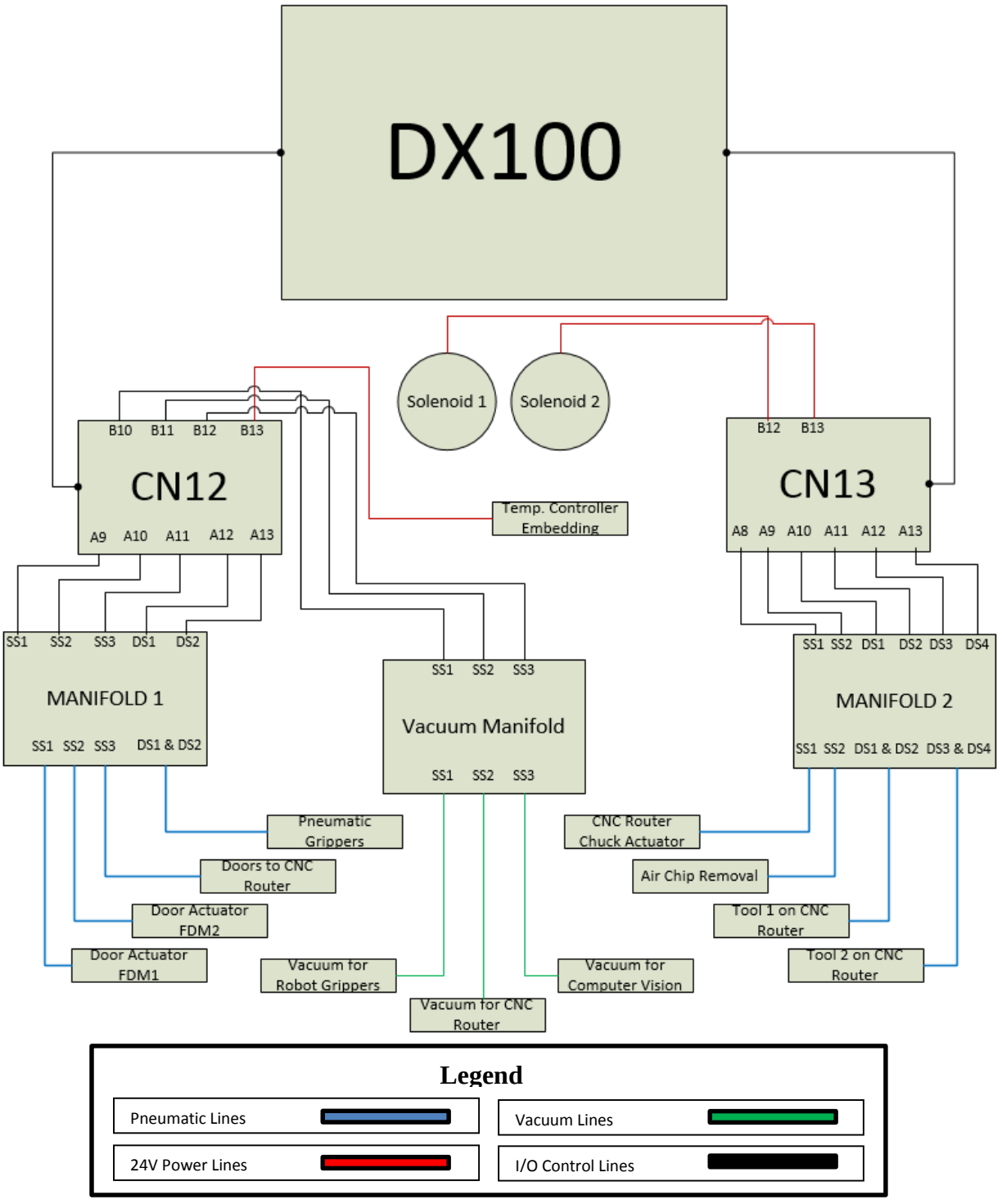

Figure 4.1. Output Diagram of the DX100 Controller

controlled by the DX100, specifically, by the ports CN12 and CN13. The Multi^{3D} System contains three manifolds, two of which are for pneumatics, and the other manifold is utilized for vacuum. The diagram shows how the manifolds were connected, as well as the components each control.

The legend provided describes each type of connection made for the controls. The blue lines represent pneumatic lines, the green lines provide vacuum, and the red lines are 24V power lined directly supplied by the DX100. The solenoid valves that will be described in the next section, as well as the temperature controller used for the traveling envelope, are rated for 24V, which is why they were connected directly to 24V. Other connections to the controller, shown in black, are the input/output lines that are controlled by the DX100. As can be seen in Figure 4.1. the I/O lines were connected to the manifolds because those were responsible for allowing air or vacuum to be activated or stopped. Through the LabVIEW programming, the ports were used to turn on the vacuum on the robot, actuate the grippers on the robot, unlock the FDM doors through pneumatic actuators, and provide various functionalities to the CNC router, including tool changing pneumatics. Aside from the I/O ports already mentioned, the DX100 also utilized ports for checking external inputs. Here, the controller constantly read values from inductive sensors, as well as other components. Specifically listed, the external inputs include the inductive sensors that signaled when the FDM doors were open, the high-temperature inductive sensors within the printers that signaled when the platform was placed, and the sensors in the solenoid interlocks that signaled if the fence enclosure was secure. The fence enclosure was made for the safety of the user, and preliminary checks were done to prevent any harm to the user, as will be described in the next section.

4.3 Safety Circuits

An initialization process was developed for the Multi^{3D} System that required user input, to determine the manufacturing stations that would be utilized for a particular build. The process deemed “Safety Circuits” operated a set of diagnostics that would prompt the user to perform tasks necessary to begin the printing process. The components were checked to determine if they were in a predetermined state, with “1” being high, or on, and “0” being low, or off. The diagnostics checked the state of the following equipment: the solenoid interlocks, Figure 4.2., the inductive sensors on both the FDM doors, and the state of the manufacturing stations. The listed equipment

Figure 4.2. Solenoid Interlocks for Safety Circuits

and the description of each status can be found in Table 4.1. Through the diagnostics being run, messages were prepared that notified the user if any of the stations planned to be used was turned off. A message also appeared if the fence enclosure was not secure and the user was prompted to lock the entrances to ensure safe operation of the robot.

Table 4.1. Diagnostic checklist

Initialization Diagnostics

Equipment	State	Description
Solenoid Interlock 1	1	Key inserted, fence secure
Solenoid Interlock 2	1	Key inserted, fence secure
FDM1 On/Off	1	Machine is operational
FDM2 On/Off	1	Machine is operational
CNC On/Off	1	Machine is operational
FDM1 Door	0	Door is not open, proceed
FDM2 Door	0	Door is not open, proceed
CNC Door	0	Door is not open, proceed

The safety circuits primarily function to avoid damaging the system if for example, the robot tried to enter a manufacturing station that was not powered and the door was not open. Other possible safety hazards include injury of the user, if inside the Multi^{3D} System while operating.

The equipment checked throughout the programmed safety circuits, gave adequate level of safety in order for verifying if the build could begin. Once the safety circuit part of the program was complete, the Menu was created as will be discussed in the next section.

4.4 Menu

The Menu function in the programming intakes the build information provided by the user, and translates that information to platform transfers. Figure (4.3) presents the steps through which

Figure 4.3. Steps describing of the Menu function

the user undergoes to prepare the Menu. The Menu function appears after the Safety Circuits have been tested. Once the Menu prompted user input (Figure 4.3.a), the user would simply select the stations, in the correct order, where the platform should be moved to. After each selected item, the user would insert that item into the sequence (Figure 4.3.b). Once all the stations to be used are inserted, the next step is to output the sequence (Figure 4.3.c). That sequence is finalized by selecting the stop button (Figure 4.3.d), causing the Menu VI to close and the program to begin with the first item on the list. After starting the system, the platform will be placed in the manufacturing station that is first selected, if not there already. High temperature inductive sensors were installed in each station to identify where the build platform is at all times in the system. The program moves the robot to remove the platform from the first station and place it into the next. This allows for flexibility in the build process in that the robot can be made to place the platform in any of the stations required to complete a build. Flexibility is crucial, as some processes might involve the use of only some of the machining stations, and some processes might require the use of the same station multiple times. While the Multi^{3D} System was running, a function was made to allow interruption of the process by the user.

4.5 Pause

The pause function was added to allow for user interjection. This would be utilized if for some reason the robot did not properly place the platform, if the grippers malfunctioned, or any other errors. The enclosure was locked throughout the entire build process, whether it be for printing or machining. For this reason, the Pause feature was added, serving as a point in which to open the interlocks to the fence enclosure and allow the user to enter without compromising safety. (Figure 4.4.) shows the steps that comprise the Pause function. As can be seen in Figure 4.4.a, the Start button is activated by the completion of the safety circuit process. The front panel showing “CNC to FDM2” pops-up, containing all the pre-set positions that are used to remove the build platform from the CNC router. The entire process can be paused at any point by the user manually pressing the PAUSE button shown in Figure 4.4.b. The light indicating the pause will be lit, and

a)

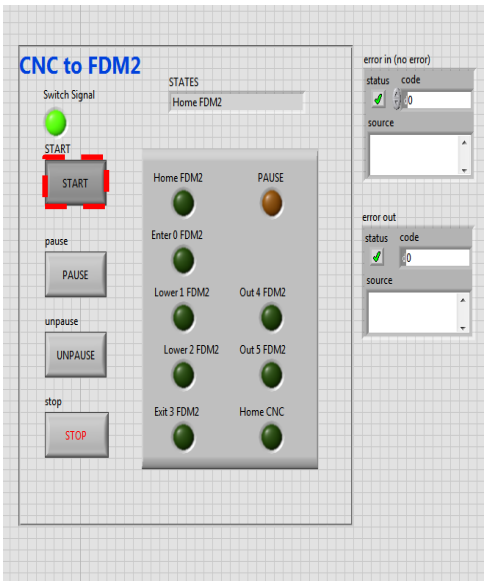

b)

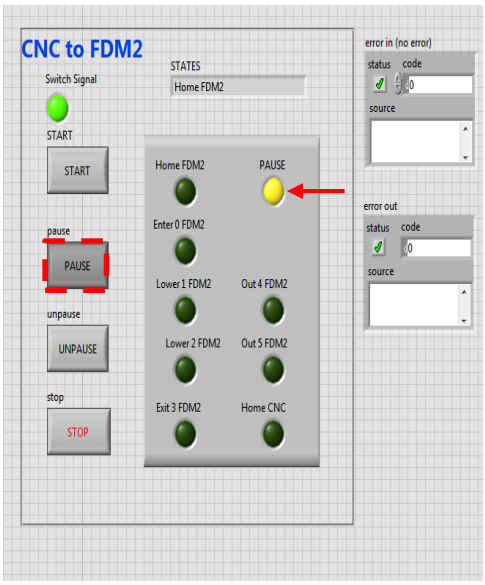

c)

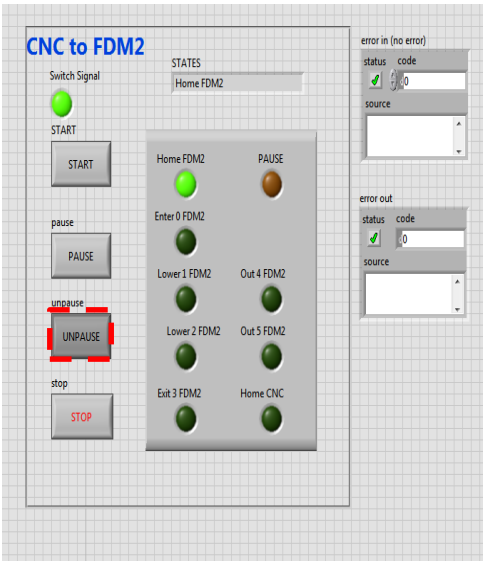

Figure 4.4. Steps describing of the Pause function

the entire system will seize to move while the interlocks will be actuated to allow entry into the manufacturing area. The robot will then remain motionless until both of the entrances have been secured once the user steps out of the area. Figure 4.4.c. shows the UNPAUSE button that will trigger a check of the fence enclosure, before resuming the process where it left off. The manner in which the positions are read by the program, selecting pause while the robot is in motion toward a position, will cause the process to be paused right after it completes its current path. This in turn signifies that once the un-pause is selected, the process will resume by continuing to the next robot

position. The purpose of the Pause function, as mentioned before, was in the event that there was a malfunction that the user can correct, and therefore would need safe entry into the manufacturing area.

Figure 4.5. shows the functionality of the pause feature added to the program. The left side of the image contains a logical converter that will determine whether at any point the user has pressed the “PAUSE” button. If the user has not, the queued message handler will send the next position for the robot to move to. If paused, the command will cause the case to change to “PAUSE”. The right side contains the cases, or different positions for the robot to move to. For each position, only the case corresponding to that position and the pause case, have content. Otherwise, there are blank cases that would only bypass the step. In Figure 4.5. the “Home FDM2” case is activated and the content shows the VI that will move the robot to that position. If pause were to be pressed, the “PAUSE” case would be activated, shown in Figure 4.6. The outer VI labeled “STATES” is made to store the value output by the “PAUSE” case. As seen in Figure 4.6., Home FDM2 was the position the robot would have moved to before it was paused. Therefore, “Home FDM2” will be stored as the state while the user desires the system to be paused. Once the user has deemed it safe to resume, the user will select the un-pause button. The program will

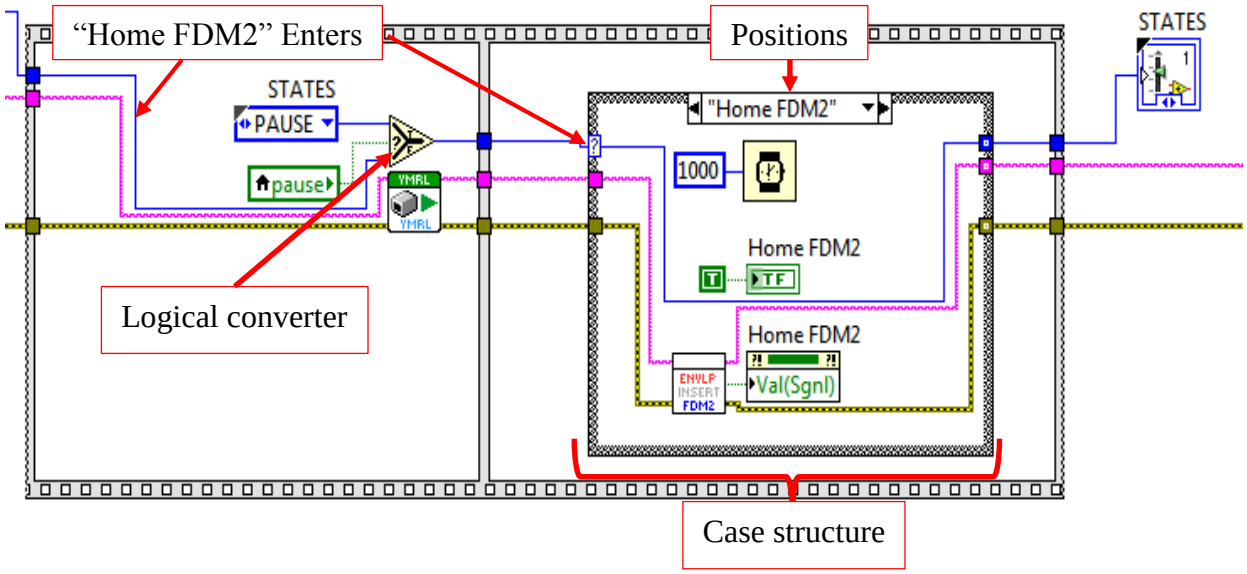

Figure 4.5. Pause feature internal structure

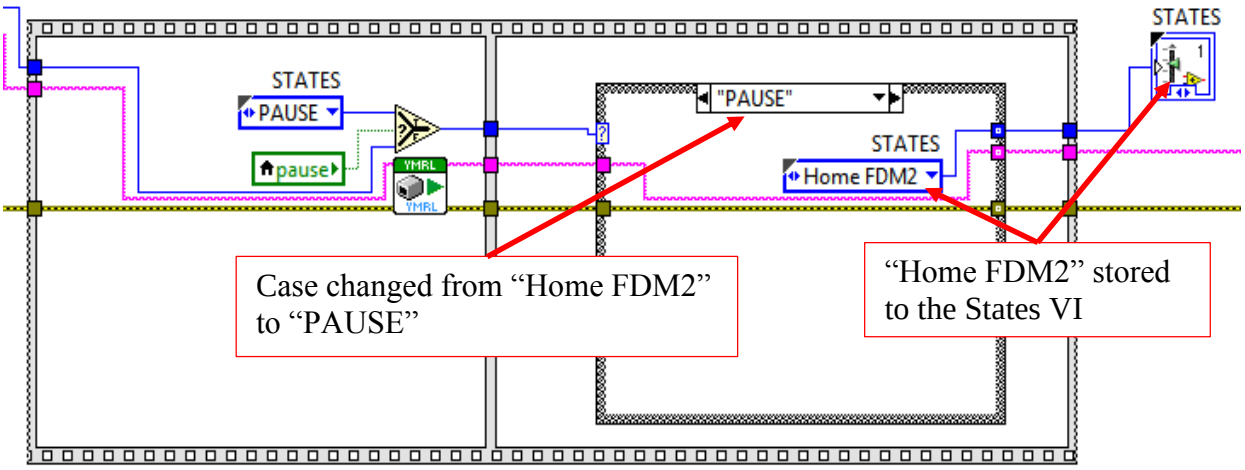

Figure 4.6. Pause storing the position to the states virtual instrument

reinitialize and the value that was stored in the states VI, will be sent to move the robot to the successive movement. Figure 4.7. shows the "un-pause" case and how everything is reinitialized and the states outputs the stored value. In the example case, because the process was paused at the Home FDM2 position, that is where the process will resume once the user unpauses the system. Once the Menu and Pause features were implemented, the next steps were to set the positions for the robot to maneuver around the build space.

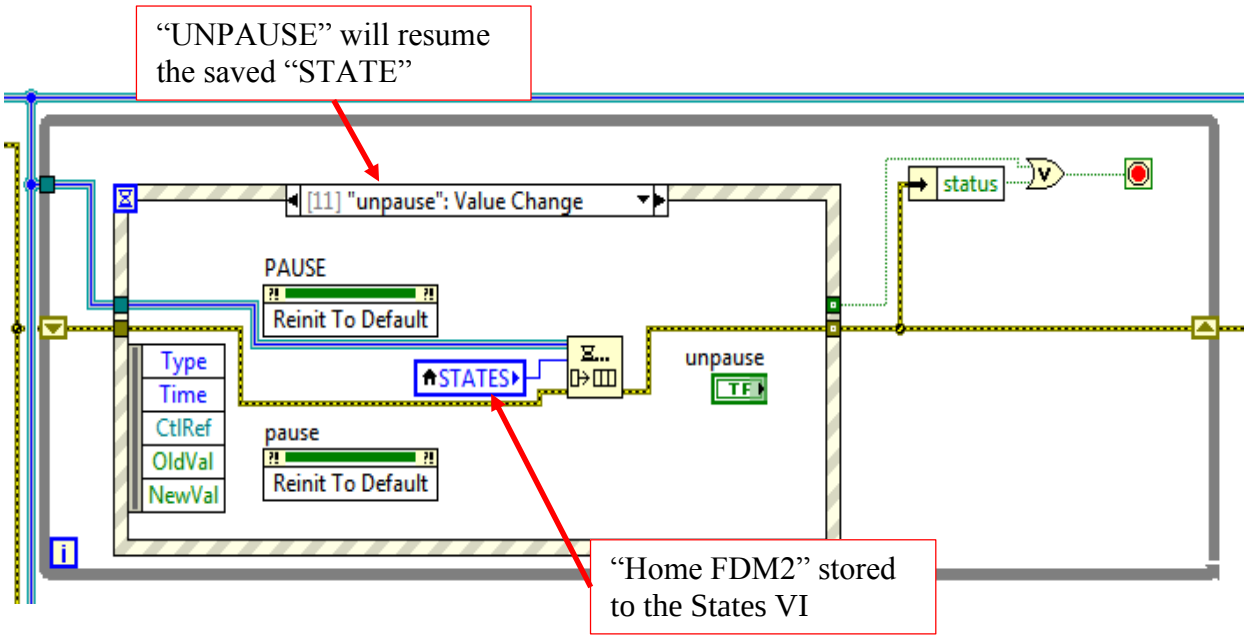

Figure 4.7. Unpausing and sending current state

4.6 Placing and Removing Travel Components

The difference between placing travel components, and removing the platform and envelope from their location, must be acknowledged because of the variance in the approach. Although placing and removing travel components utilizes the same coordinate positions albeit reversing the direction, there are other parameters that require further inspection. Understanding the method of both placement and extraction brings forth the reasoning behind the methodology implemented in each separate process. The material handling robot, material referring to the portable build platform, receives positions that are sent specifically for what is to be accomplished. At the initialization of the system, the portable build platform will be located inside any of the manufacturing stations. The removal of said platform from the FDM printers is illustrated in Figure 4.8. There are differing number of points for the removal of the platform depending on the station. For any motions within the FDM machines or the CNC router, there are a total of six positions. The table where the travel envelope is placed when not in use contains only five positions. The addition of a sixth position for the FDM machines is meant to accommodate the small tolerance of 3.175 mm (1/8”) that is allowed on either side of the travel components during the extraction of

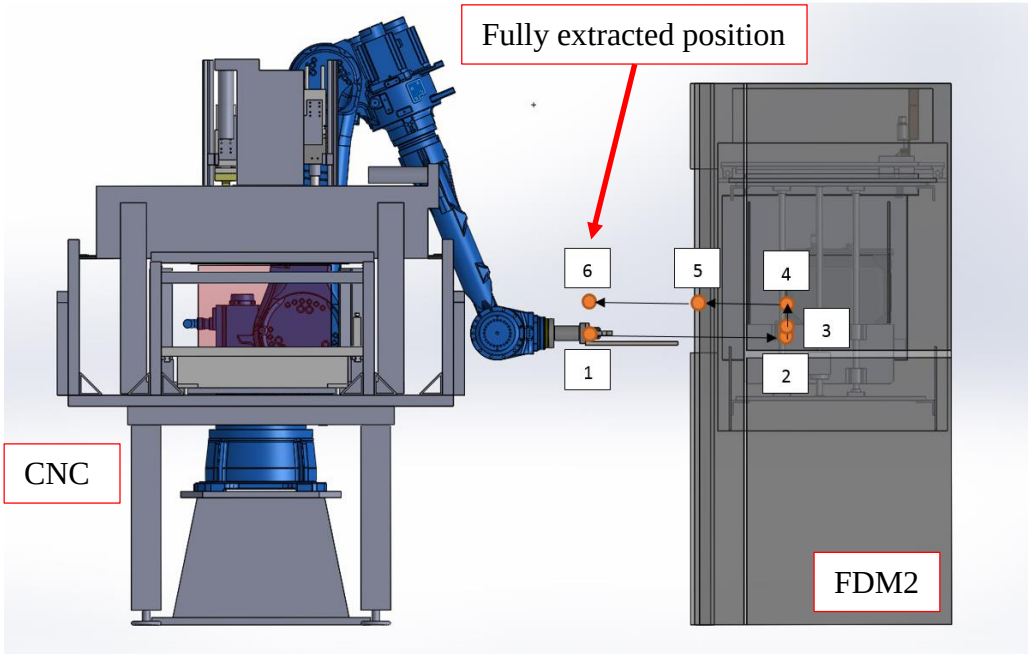

Figure 4.8. Positions for Placing and Removing Build Platform

both the platform and envelope. Figure 4.9. shows position five that is added between the top position inside the FDM and the fully extracted position. As can be seen, there is very little tolerance between the traveling envelope and the entrance of the FDM. This was designed to maximize the build volume of the portable build platform, however, the robot is slightly shifted in this intermediate point to allow for the envelope to be extracted without collision. The table upon which the envelope is housed, poses no risk of collision based on the width of the envelope, allowing for the removal of the intermediate point.

As previously mentioned, the positions for placing and removing any of the objects within the Multi^{3D} System are the same, but the approach is different. The primary reason for this change is the speed of approach. Due to the nature of reversing the direction of motion, some of the distances are further in one direction than the other. For example, the distance in Figure 4.8. from position 1 to 2 (609.6 mm) is much greater than that of position 3 to 2 (38.1mm). Therefore the speed to get to position 2 is much faster when removing (approaching from position 1: 87.1 mm/s)

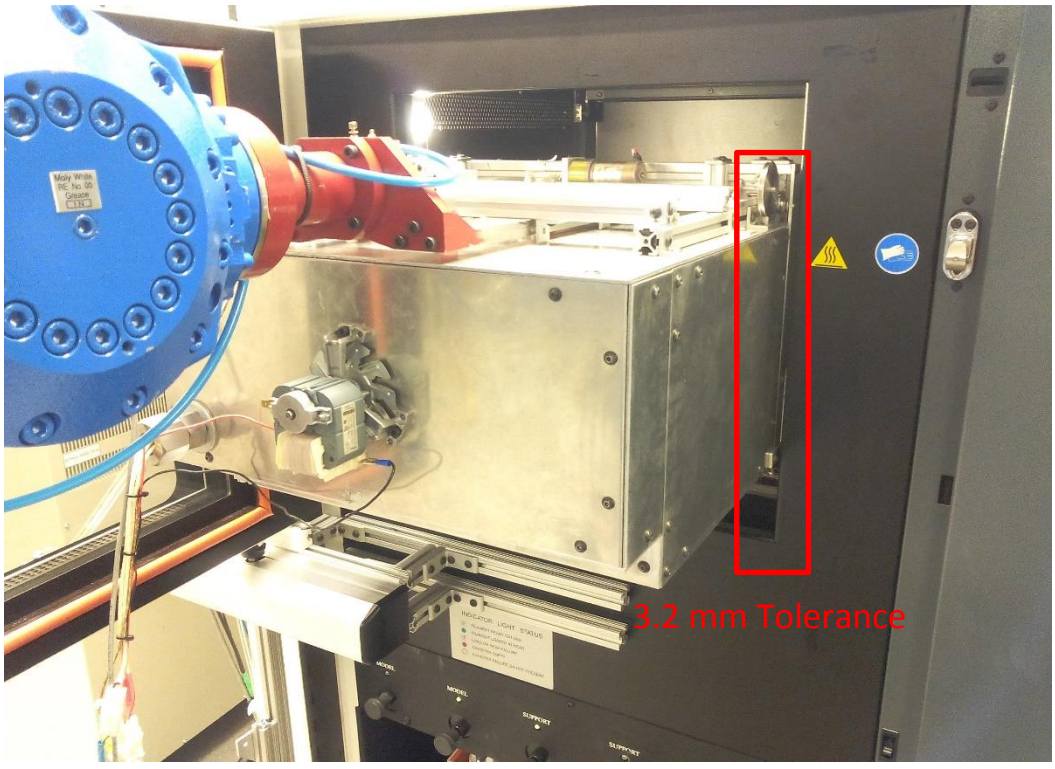

Figure 4.9. Position 5 in the placement of the traveling envelope

than when placing (approaching from position 3: (12.7 mm/s). This led to the utilization of two separate VI's to get to the same position, that are distinguished by the speed of approach and also the type of motion (linear or synchronized). The difference between the types of motion is that linear motion is a direct linear path of the end effector from one point to the other, and synchronized motion disregards any set path and simply moves the robot from one point to the next. The synchronized motion typically results in arching motion that would cause a collision if it were to be used when maneuvering inside the manufacturing stations. Synchronized motion is almost exclusively utilized when the robot is getting to its position outside any of the manufacturing stations. Since two VI's were created for each of the positions the robot moved to, every change to the coordinates of that position required the locating of the VI's that utilized those coordinates, and manually inputting the new pulse values on both VI's. Changing one and not the other would result in the travel components being either placed or removed incorrectly. The method for inputting the coordinate values will be discussed in the next section, as well as the second iteration to acquiring values.

4.7 Position Coordinates

The methodology implemented in the capture of the positions required to perform the robotic motions will be addressed. Initial acquisition of the coordinates involved the user manually positioning the robot in the desired location. The control panel displays the number of pulses that

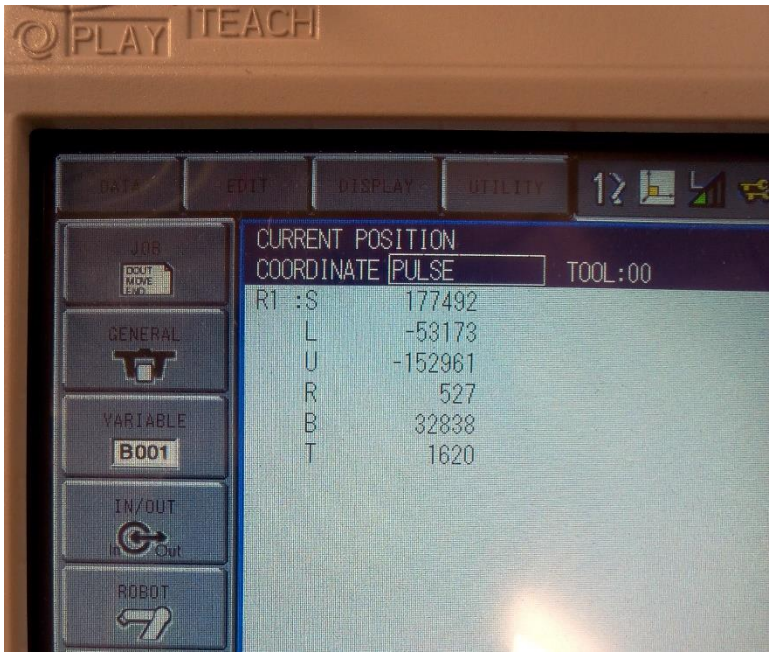

Figure 4.10. Pulse coordinate display on handheld control panel

each of the axes have rotated to reach the current position. These values given as shown in Figure 4.10., have all the values in order from the base (S) to the rotation of the tip of the robot (T). Pulses were recorded and the VI's that correspond to that position would be changed to the new location.

The VI that was utilized for all the positions of the robot throughout the Multi^{3D} System is shown in Figure 4.11. Note that within this VI the pulses, speeds, and accelerations for each servomotor as well as type of motion were specified. This VI requires that the programmer input pulse values manually. Additionally, the robot session and error are important inputs and outputs for each VI because through the identification of the robot session, the motion can be sent to the DX100 controller. The error line runs throughout the majority of the programming sequences because any error that is encountered in any part of the system's motion will be identified and

prevent the program to continue. This avoids possible collisions if the robot were to move into a position that was not prepared to receive it.

The method of manually inputting pulse values was replaced through further understanding of the programming. The final method of acquisition of the coordinates involved manually setting the robot in its position, however, the recording of the value and the insertion into the proper VI's was greatly simplified. A VI able to attain the position of the robot directly, was utilized, along with a VI that could set that particular set of values, to replace any desired position. This method was particularly helpful as much of the project involved constant changing of the coordinates to accommodate for error and misalignment of the system. This misalignment was due to changes in temperature and even collisions. Figure 4.12. shows the simplification of each VI when compared to the initial method of inputting coordinates. As can be seen from comparing to Figure 4.11., the individual pulses were replaced by a single digit that corresponds to the position the robot will

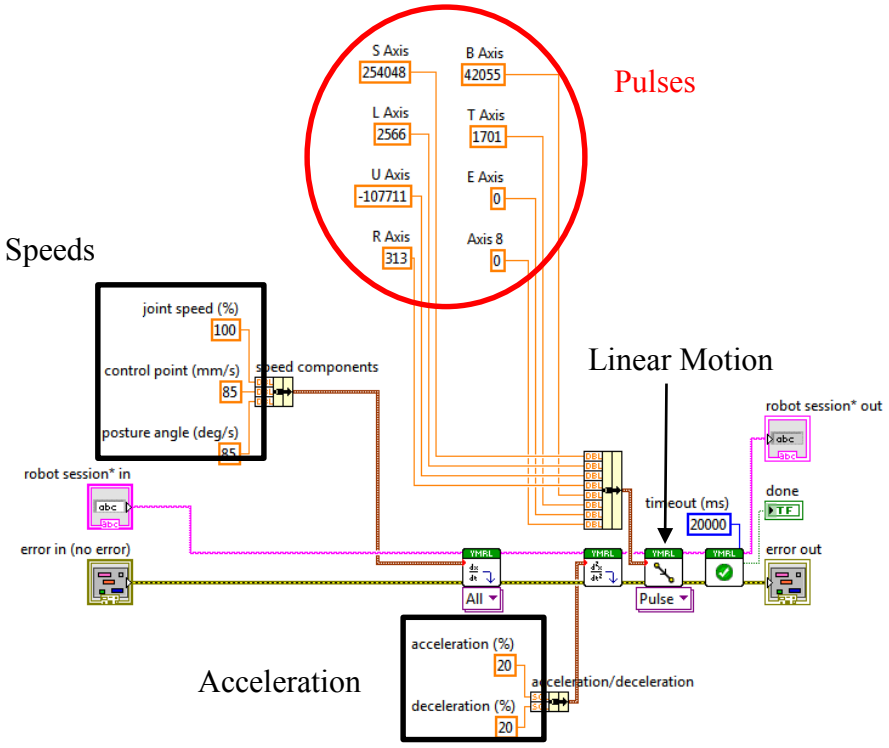

Figure 4.11. Initial method of inserting coordinates via pulses

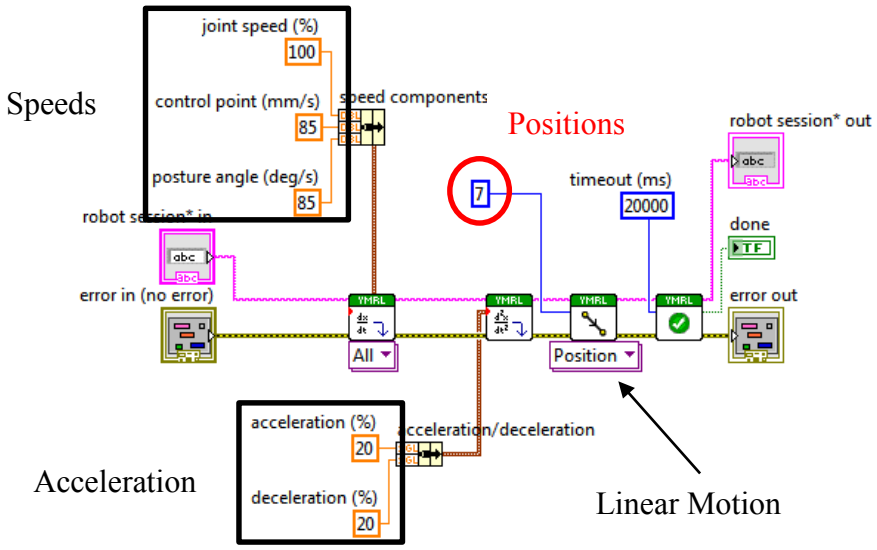

Figure 4.12. Final method of inserting coordinates via positions

move to. In Figure 4.13., the methodology is demonstrated for replacing a position. On the left, the "Get Position" VI is represented, where running it automatically outputs the coordinates to the user of the robot's exact location at that point in time. It is noted that because the Yaskawa MH50

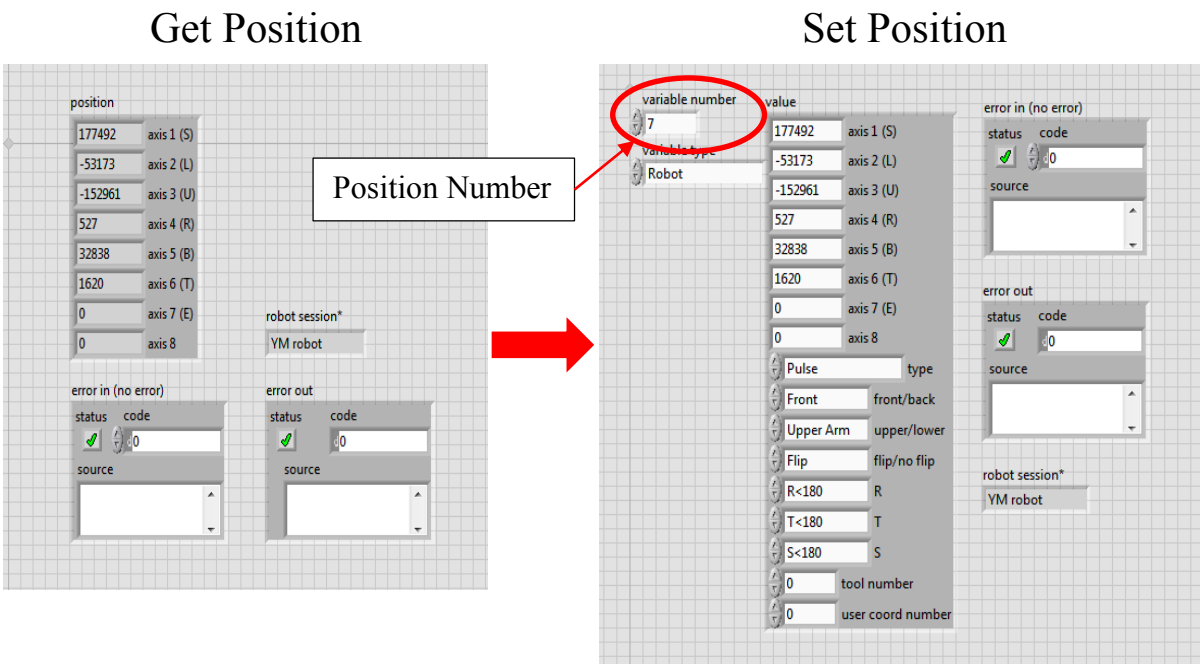

Figure 4.13. Getting and setting coordinate panels

is a six-axis robot, the seventh and eight axes print a value of zero. In the same figure on the right, the "Set Position" VI is shown. The user identified which was the position that needed to be replaced, move the robot into that new position and retrieved the value. Then, those values were transferred to the "Set Position" and the desired position was saved. Finally the VI stored the pulse values in a database allowing the LabVIEW environment to correct any motion VI that referenced that position. One important note is that the positions stored must be distinct, making it necessary that the numbering of the positions be determined beforehand based on the motions expected by the robot.

Figure 4.14. provides a schematic for the position programming of the robot. The black arrows represent the direction of the robot's motion for removal of either the build platform or the traveling envelope, for each of the stations they interact with. The red arrows cycle in the opposite

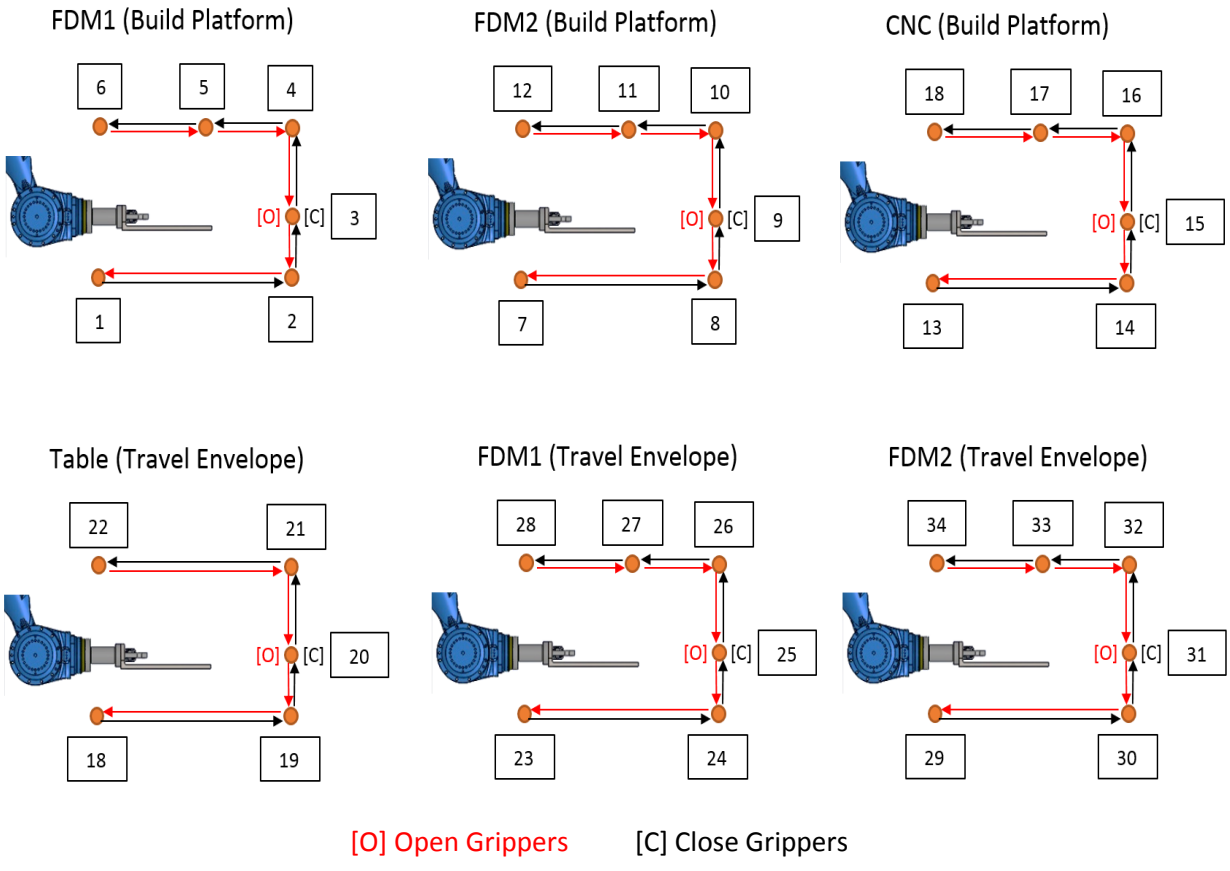

Figure 4.14. Established positions for the robot

direction, showing the motion for placing. As mentioned previously, there is a position in-between the top positions in most of the VI's to allow for some shift during the entrance of the robot into any manufacturing station. Also, there are symbols representing either the opening or closing of the grippers when at the designated position in each cycle. This position is the one at which the platform or envelope are exactly in position on the station. This is the ideal location to grip onto either component before lifting, or to open the grippers before lowering the forks out of the way. An example of the positions that are obtained then set in the program is shown in Table 4.2. For the testing that has been completed thus far, the positions that are utilized are those that involve the FDM2, which has been modified first. Therefore, positions 7-12 are used to place and remove the platform, and also the positions 29-34 to place and remove the envelope from atop the platform. Positions 18-22 are used to position the travel envelope atop a table when the envelope is not being used. As can be seen from the figure, the travel envelope to the table it rests upon, involves only five coordinate points. This is because there are no obstructions at the envelope table, meaning there is no possibility of collision with an entryway.

Table 4.2. Positions 7-12 for FDM2 from Pulses

FDM 2 (Platform)	**Pulses for Each of the Six Axes**					
Position	S	L	U	R	B	T
7	253781	-1071	-111646	488	41833	1449
8	254004	41167	-46791	368	37098	1473
9	254005	41034	-46753	368	37021	1474
10	254004	39286	-46190	370	35975	1470
11	253988	11124	-91255	353	39826	1493
12	253693	-39850	-144274	602	35857	1374

It is expected that coordinates (pulse values) will be obtained for the predetermined positions, and that other positions will be added once the computer vision station is established.

As mentioned in Section 4.6, the speed between each point varies depending on the direction of the cycle, either placing or removing. A table with all the utilized positions can be found in Appendix A.

Chapter 5

Results

5.1 Mock FDM machines

The arrival of the robot brought about the opportunity to begin validation of the component placement. The floor was marked where the robot was to be placed, with the correct distance between its center and the wall. The distance allowed for the FDM2 to be placed with a 21.25" (540mm) gap between itself and the wall, allowing for user maintenance on the 3D printer. Once the robot pedestal was installed, the robot was lifted and fixed onto the base. The floor was marked, 58" from the center of the pedestal, in all directions to mark the position of the manufacturing stations. Although the 3D printers had already arrived by the time the robot was in place, the risk of damaging them by inexperience with the robot controls prompted the construction of what were called Mock FDM machines. Figure 5.1. shows one of the two Mock FDM machines that were created to replicate the authentic 3D printers. The Mock FDM machine in the figure was dimensionally accurate and contained an opening door, and an interior structure resembling the

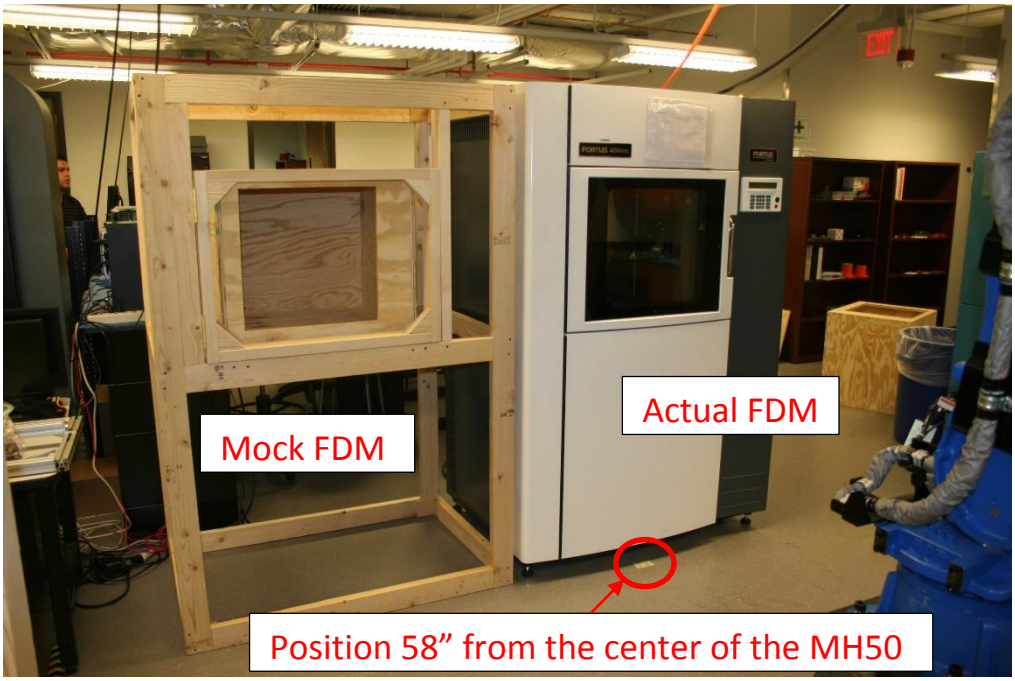

Figure 5.1. Mock FDM machines for robot testing

inside of the 3D printer. As mentioned previously, inexperience with the robot led to the construction of the Mock FDM machines for introduction to the programming controls. Since the Mock FDM machines had an entrance that was the exact dimensions of the printer, training resulted as a method to confirm that the dimensions of the platform and envelope were viable. Figure 5.2. presents the setup of the two 3D printers directly across from each other, as well as their replacements. Practice with the Mock FDM machines resulted in the development of methods that were later implemented on the actual FDM machines. This includes the benchmark positions from which the final positions were later determined, as well as modification to the build platform and grippers that allowed for improved transfers between manufacturing stations.

Preliminary testing of the robotic controls involved the movement of the robot without an end-effector. The robot was made to approach the Mock FDM, enter the envelope of the Mock FDM machine, simulate the placing or lifting of an object, and finally retracting from the Mock FDM machine. The approach was based on the eight tasks for transferring an object between destinations (Sayler & Dillmann, 2011). Once the manufacturing of the grippers was completed, the testing resumed with the use of the build platform.

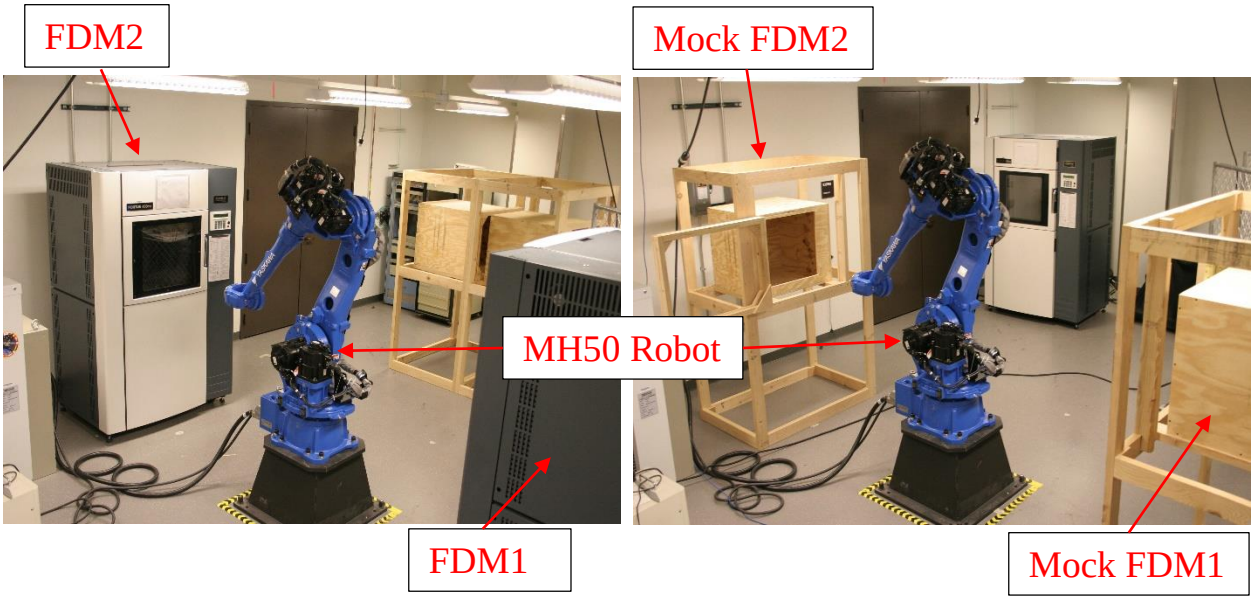

Figure 5.2. Mock FDM Machines replace Actual FDM machines for initial testing

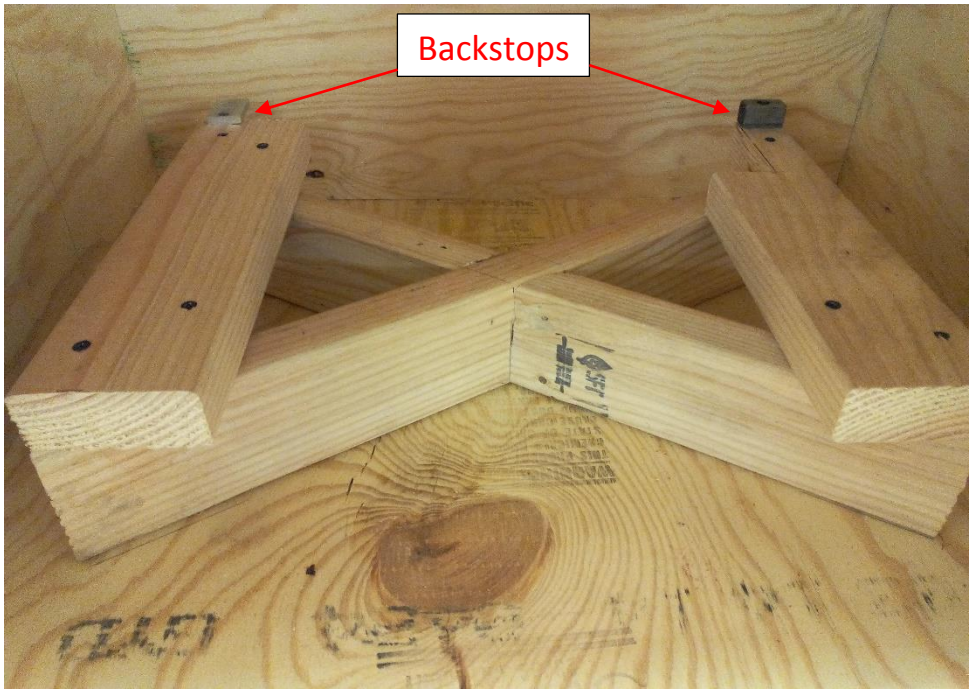

Figure 5.3. Backstops within the envelope of Mock FDM1 to prevent backward motion from the platform

A wooden stage was constructed to simulate the height of the placement of the portable platform. It was installed in Mock FDM1 as seen in Figure 5.3. Attempting to attach onto the platform with the grippers was not successful. When the robot entered to remove the build platform, the friction between the forks and the platform would cause the grippers to incorrectly engage around the gripping block. Backstops were added to the mock structure, Figure 5.3., that would prevent the backward sliding of the platform. This simulated the effects of the stability added by the locating pins, which were installed on the modified interior of the actual FDM machines. By preventing the shift of the platform, the robot was able to successfully and repeatedly remove and place the platform in the same location, as later results will show. By design, the locating pins were meant to restrict the movement of the build platform when coming in contact with the end-effector, ensuring the repeatability of the program. The Mock FDM machines were used for much of the initial tests, and led to the verification of some design changes, and the safety of the actual FDM machines.

5.2 Modifications triggered by the MH50 robot

The application of the robot contributed significantly to the design of multiple components of the Muli^{3D} System. From initial testing of the contact between the pneumatic grippers and the portable build platform, it was determined that the platform was steadily sliding forward (away from the grippers) during transport. The experimental procedure of the gripper test consisted of attaching to the portable platform with the robot, and placing the platform inside Mock FDM1. Then, the platform was returned to a position over a table (Figure 5.4.), upon which a MICROTRAK 7000 Laser displacement sensor was attached. The laser displacement sensor was placed in two different positions for the testing of the portable build platform. Position one (back position), is near the center-point of the outer edge of the platform, the side that enters first into the manufacturing stations. Directly across the end effector, position one was monitored to determine linear movement with respect to the forks on the end effector. Position two (top-left position), was chosen to monitor any rotation of the platform, which would result in the misalignment and possible collision when inserted into the 3D printers. Given that the robot is repeatable to ±0.07 mm (±0.003”), the MH50 was tasked with having the platform hover over the position seen in the figure (Motoman, Yaskawa Motoman Robotics, 2012).

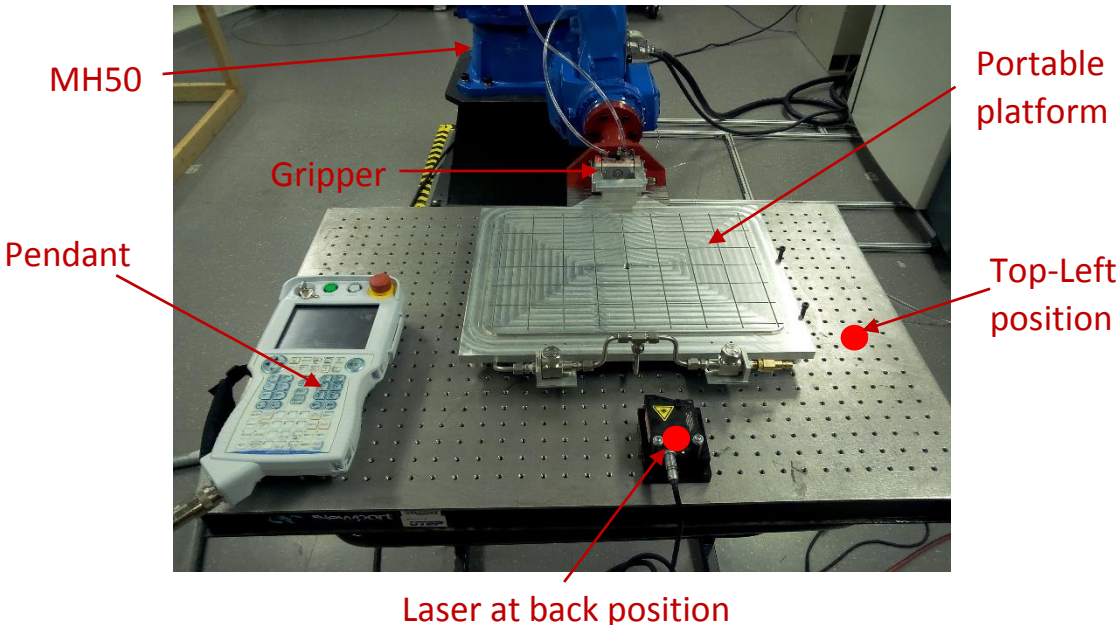

Figure 5.4. Experimental setup for laser displacement sensor

A program was created with LabVIEW that would repeat a set order to commands in order to execute the testing of the portable platform shift. The experiment consisted of the following steps. Initially, the platform was gripped by the end effector at a set “Home” position, hovering over the table in Figure 5.4. The robot was then programmed to lift the platform, rotate to the Mock FDM1 machine, and place the platform onto the wooden stage. The grippers were opened, and the robot was retracted, completely placing the platform as would be done in the final version of the program. The robot was then able to enter the Mock FDM1 machine, grip the platform, and return it to the previously mentioned “Home” position, where a distance measurement was given by the laser displacement sensor. The sensor was given one minute to stabilize its reading before the distance was recorded. The values were recorded for the ten iterations conducted on each of the two positions. The results led to the identification of design changes to the manner in which the grippers attached to the platform, and led to the addition of alignment bars.

The first of the modifications that were made resulting from the laser displacement tests, was the introduction of alignment bars to the build platform. Data collected from the two positions

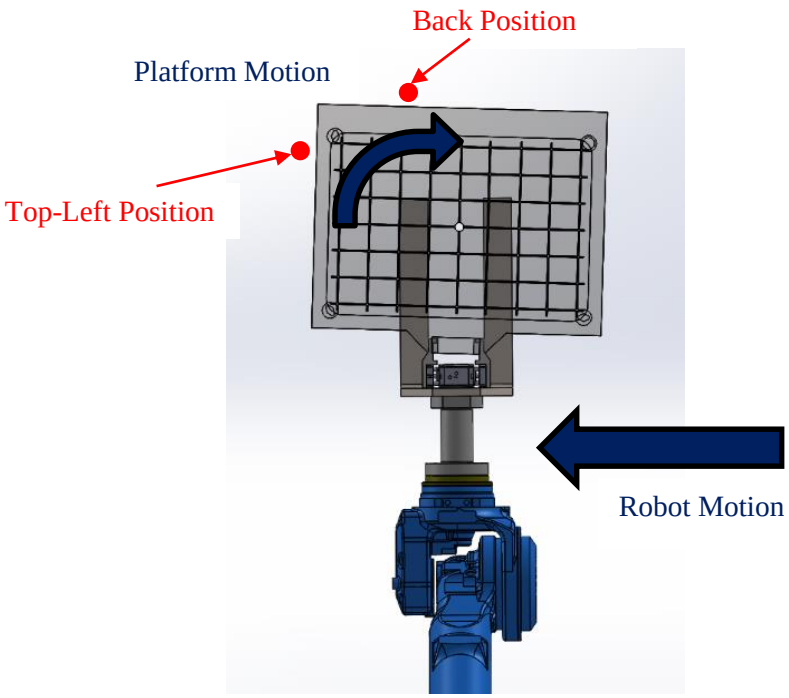

Figure 5.5. Platform Shift without alignment bars

provided the following conclusion: the grippers were not sufficient to prevent the rotation of the platform as it was being transported between stations. Figure 5.5. exhibits the shift in the platform consistent with the values obtained from the laser displacement, which can be found in Appendix A. The table of values show that over ten iterations, without the addition of alignment bars, the back position shifted by a maximum of 1.295 mm with a standard deviation of 410.5 µm. Repeating the test with the top-left position, the maximum shift over ten iterations was determined to be 0.398 mm with a standard deviation of 176.0 µm. Considering the test was conducted for each of the two laser sensor positions separately, there is no correlation between the two sets of data. However, the results show the distance from the platform to the back position is consistently decreasing. Contrary to that change, the values for the top-left position increased throughout the experiment. When joined, the results serve to confirm that the platform was shifting due to the rotation of the robot arm, Figure 5.5., and a means of limiting that shift needed to be identified. As a result of the shifting, alignment bars were introduced to prevent the movement caused by the rotation of the robot. The bars were placed on the bottom of the build platform, in such a way that the forks would keep the platform parallel to the end effector. The alignment bars are shown in Figure 5.6., along with the placement of the platform into the Mock FDM machine. After the

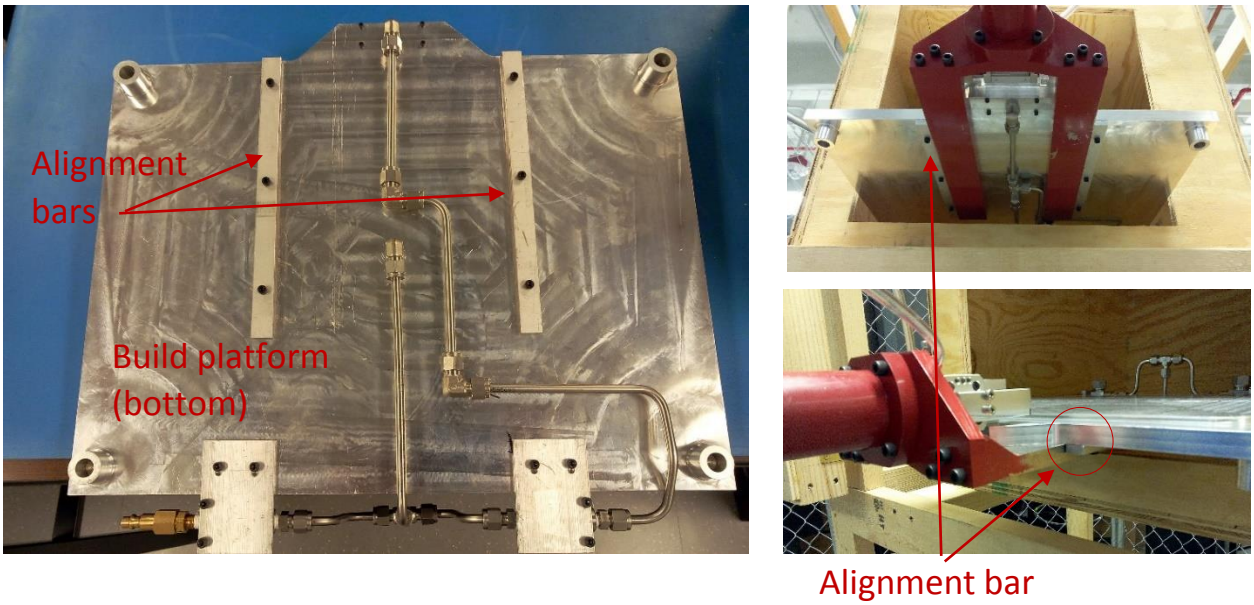

Figure 5.6. Addition of the alignment bars for reduction of inaccuracy

modification, secondary tests gave the conclusion that although still fluctuating, there was an improvement. Results showed a reduction of the standard deviation between the two sets of data, with and without alignment bars. The percent reduction for the back position was found to be 19.23% and that of the top-left position to be 8.78%. The reduction of the standard deviation, signaled the increased precision of the placement. However, after continued testing, another modification was made to the system that resulted in increased repeatability in the placement and removal of the platform in Mock FDM1.

Even after the addition of the alignment bars, it was apparent that the distance between the platform and the laser in the back position was still decreasing. This is attributed to the fact that while the robot was rotating, some of the rotational motion was translated to linear motion, in this case, sliding the platform forward. To correct the linear motion the grippers were redesigned to include a feature that allowed for the alignment of the platform to be more consistent. The initial and final design for the grippers can be seen in Figure 5.7. A circular pin was added to the grippers, along with a notched gripping block on the platform to allow for better mating and to prevent the sliding of the platform throughout the motion of the robot. The testing that was conducted after the modifications validated the changes, as the results were improved. The comparison between the grippers with and without pins can be seen the Table 5.1. The values were given by the laser displacement sensor measuring the distance from the laser to the platform at the back position. From the data, the addition of the circular pins allowed for the platform to be placed and removed

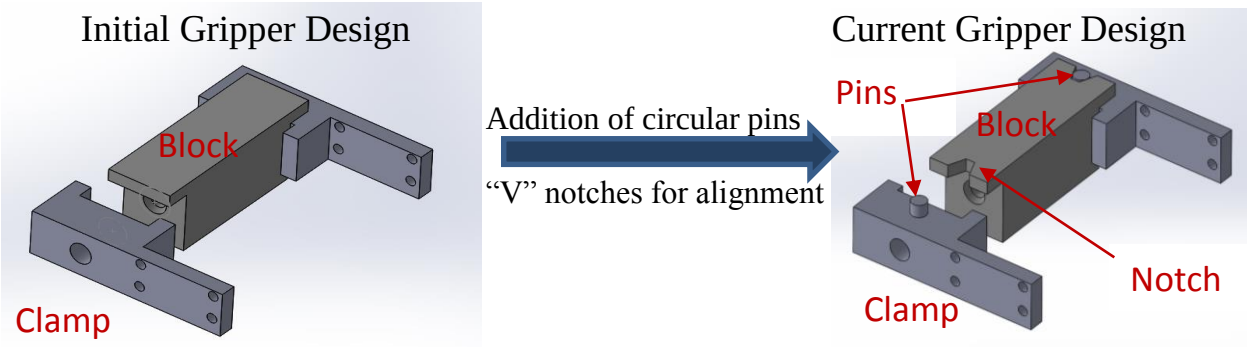

Figure 5.7. Gripper design change from robot testing

Table 5.1. Data from the addition of pins to the grippers

Trial Number	Grippers (No pins)	Grippers (Circular pins)
1	5384.5 µm	4274.0 µm
2	5252.0 µm	4255.0 µm
3	4351.0 µm	4219.0 µm
4	4218.5 µm	4249.5 µm
5	4348.5 µm	4257.0 µm
6	4259.0 µm	4263.5 µm
7	4387.5 µm	4239.5 µm
8	4325.5 µm	4262.0 µm
9	4439.5 µm	4242.5 µm
10	4432.5 µm	4231.5 µm
Average	4539.9 µm	4249.4 µm
Standard Deviation	395.7 µm	15.6 µm

with increased accuracy. From the difference between the first and tenth trial number, the shift for ten placement operations can be compared pre and post pin addition. Before the addition of the pins, the total shift after ten placements was 952 µm. After the circular pins were used, the shift was only 42.5 µm, which is a reduction of 95.5% offset. Comparing the values of standard

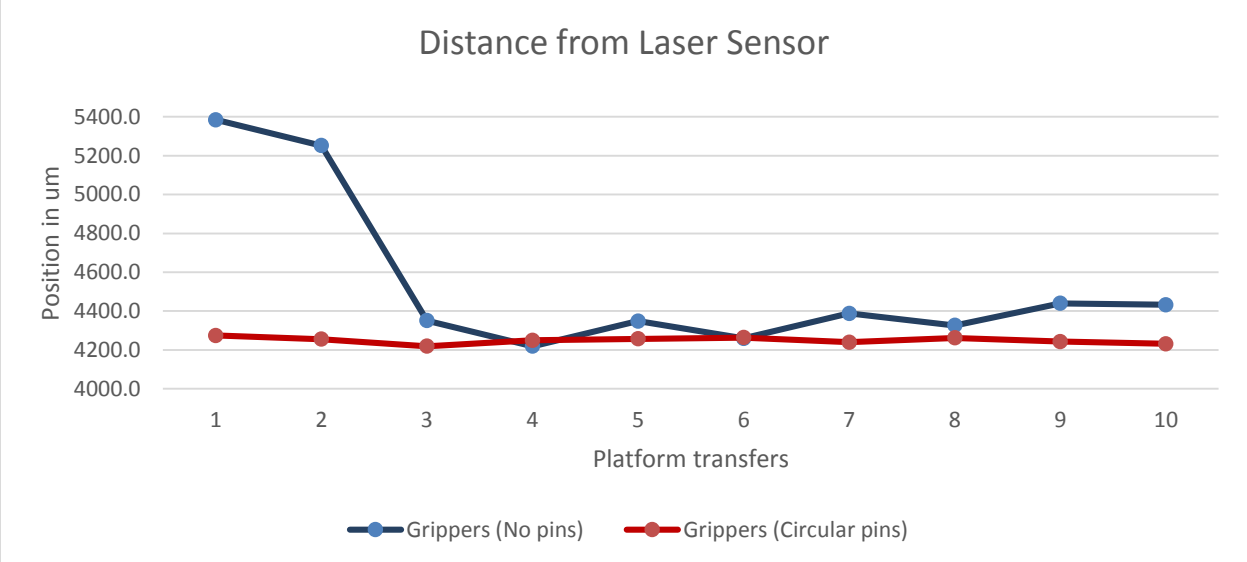

Figure 5.8. Graph of the displacement of the build platform

deviation for each set of values, a change from 395.7µm to 15.6 µm, gives an offset reduction of 96.1%. Figure 5.8., gives a visual representation of the consistency arising from the modifications to the grippers.

Once the traveling envelope was constructed to the point where it could be transferred with the robot, testing was done to determine any modifications. The laser displacement test was applied to the envelope as seen in Figure 5.9. Similar results were expected to that of the build platform. The envelope would predictably shift laterally and slightly forward. In anticipation of the causes of misalignment, modification made to the envelope included the notching of the gripping block, and the addition of alignment brackets, shown in Figure 5.10. The results from the ten iteration laser displacement test are detailed in the Appendix A. Highlights of the results include the following: seven of the ten measurements were within 0.001 mm. The highest offset was found in the seventh measurement, with the maximum shift of 1.073 mm. It was one of only three measurements that were not consistent with the others. This can be attributed to the absence of a backstop for the envelope that allowed it to slide very minimally on the wooden stage. However,

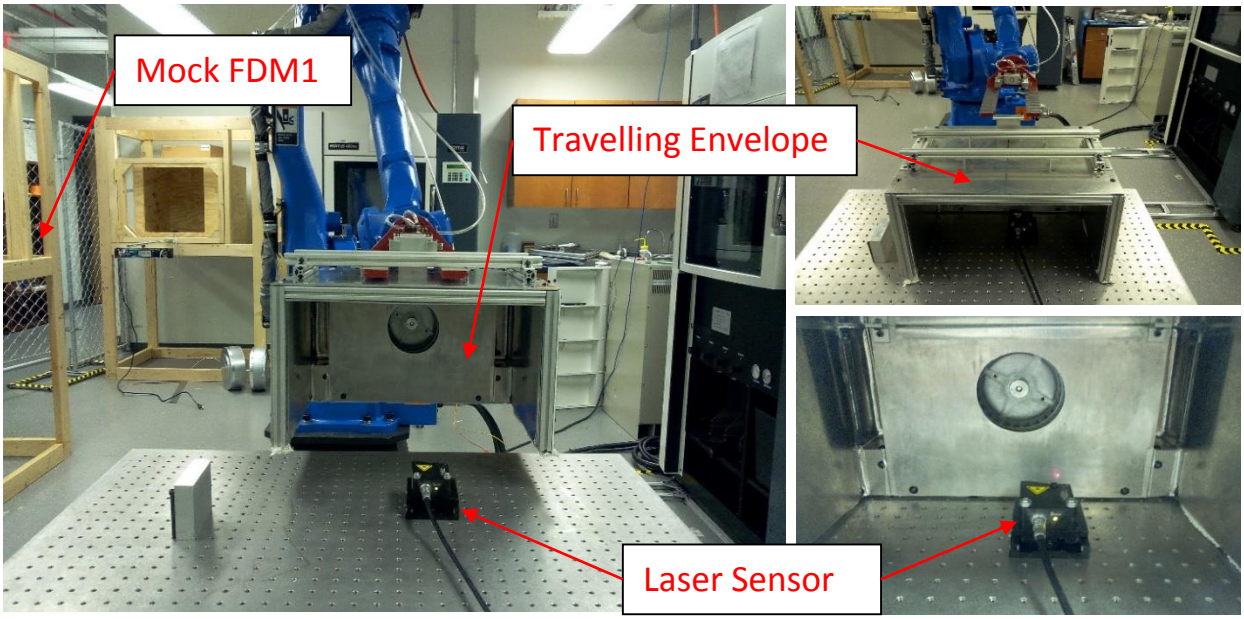

Figure 5.9. Laser Test for Traveling Envelope

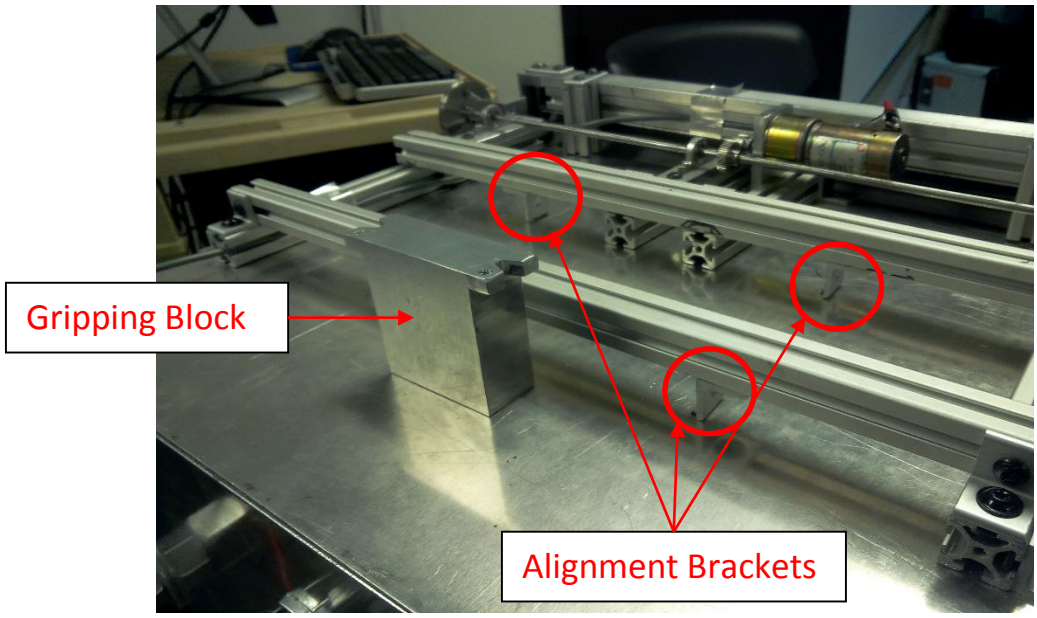

Figure 5.10. Modification to the Envelope

the conclusion of the results show the offset was removed on the next cycle when the gripper pins pulled the envelope back into place. The test confirms the improvement of the overall system by adding the notches to the gripping blocks, and the addition of alignment bars and brackets to prevent lateral shifts.

After completion of the modifications to the portable components of the system, the focus shifted to the interaction between them and the actual FDM machines. The Mock FDM machines were replaced by the actual printers. To proceed further, the manner in which both the portable build platform and the traveling envelope interacted with the FDM systems, required modifications to the interior of the printers. A leveling plate was constructed, upon which the platform would be placed over to allow printing. To maximize the accuracy of the placement by the robot, there were locating pins inserted, shown in Figure 5.11. The locating pins prevent the platform from shifting during the build, allowing for small inaccuracies to be removed. Once the leveling plate was installed, testing was done to attempt placement and removal of the platform into FDM2. FDM1 was left unmodified. It is noted that other modifications were made to the interior of the FDM machines including the vacuum port that provides vacuum for the build sheets when 3D printing.

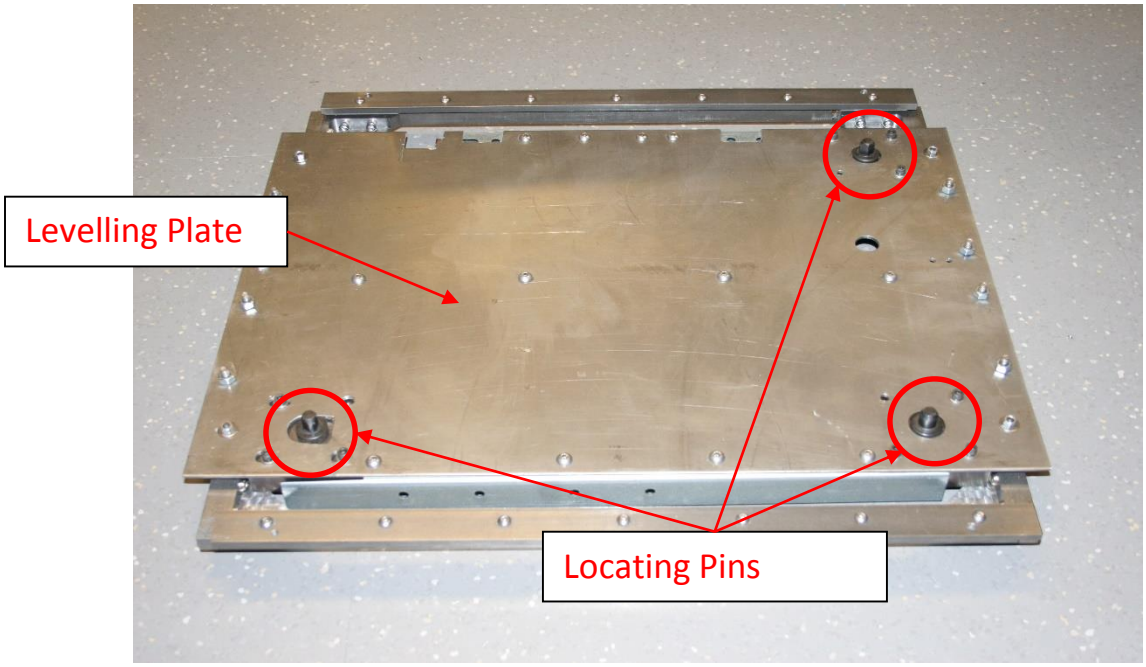

Figure 5.11. Locating pins on the levelling plate

After several attempts at placing the platform, positions were recorded on the LabVIEW environment. Next, testing was made to validate the program, by ensuring repeatability in placement and removal. Once an operational program was completed, printing with pauses began. The following test presents the results of a stair step test, where pauses were used to allow for robot platform transfers to occur.

5.2 Stair Test

To prove the concept of modifying the current Fortus 400mc systems, into those that will have the portable build platform necessary to complete the project, a stair test was conducted. The purpose of this experiment was to establish a comparison between an unmodified 3D printer, referred to as FDM1, and the modified 3D printer, FDM2. The modifications made to the printer included the installation of an entirely new leveling plate that contained the locating pins on which the build platform will be placed. The locating pins allow for precision of the placement, resulting in accurate builds. There were four prints that were conducted, to analyze the variance in the accuracy of the layers being built. The design of the part to be printed was that of a three step stair. The base of the stair step was 50.8 x 50.8 mm (2” x 2”) with a height of 19.05 mm (0.75”). The

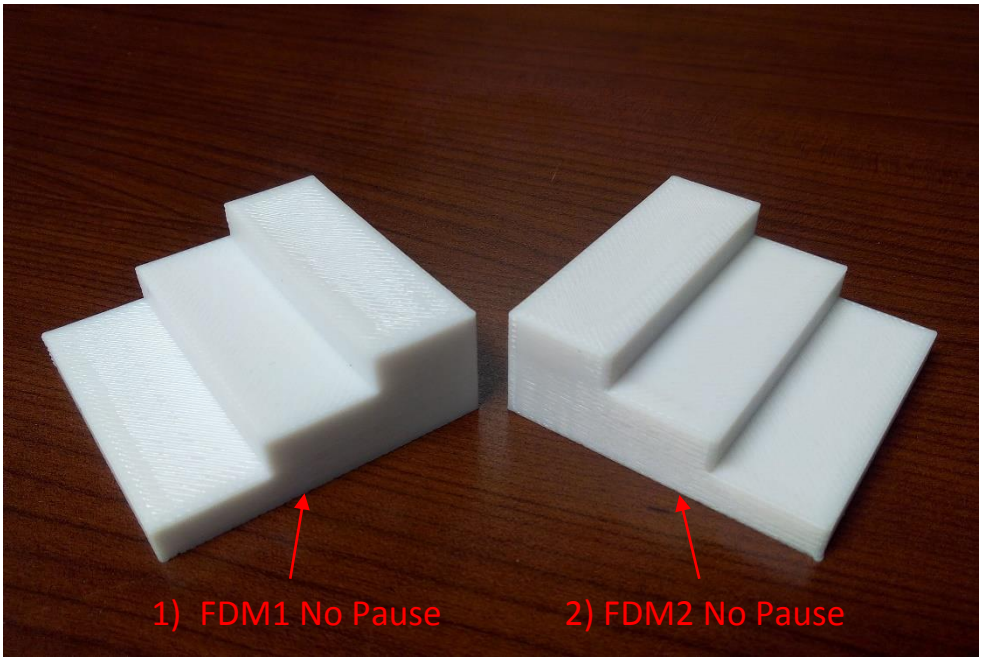

Figure 5.12. The printed steps without pauses, FDM1 (Unmodified) and FDM2 (Modified)

steps are each 16.33 mm (0.67”) long and 6.35 mm (0.25”) high. The build was seventy-five layers high, twenty-five layers per step, with a layer height of 0.254mm (0.01”). The four prints are as labelled as follows: (1) FDM1 No Pause, (2) FDM2 No Pause, (3) FDM1 Pause, and (4) FDM2 Pause. As previously mentioned, FDM1 is the unmodified printer. Stair step (1) was printed first without interruptions. Stair step (3) was done at a later time. It involved adding pauses through the Insight program, as well as the following steps. Once paused, the Stratasys manufactured build platform was moved to the z bottom of the FDM1 printer, then printing was resumed. This prompted the factory made platform to be raised to the printing tip and resume the print. Printing on FDM2 involved a very similar procedure. Stair step (2) was printed directly. The comparison between the steps on FDM1 and FDM2 with “No Pause” can be seen on Figure 5.12. The final stair step (4) was the most complex, as it involved pausing the print, having the robot removed the build platform completely, then place it on the locating pins, before resuming the print.

In order to study the results and get reliable conclusions, all of the layers of each part were measured using an optical and multisensory 3D dimensional measurement machine (OGP SmartScope Flash 250, Optical Gaging Products, Rochester NY) placed in the OGP. This device

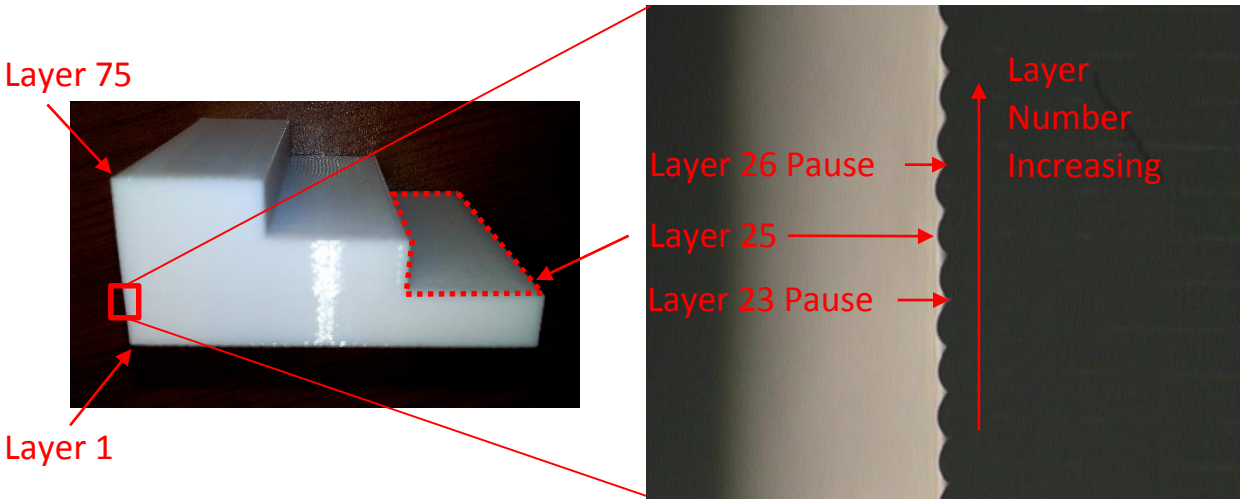

Figure 5.13. Orientation and image capture with the measurement machine 2) FDM2 No Pause

utilizes a high precision camera able to zoom and capture the shape of each individual layer printed. One of the images captured on the measurement machine can be seen on Figure 5.13., focusing on the layers that are printed before and after the transition into the second step. As seen by the figure, the layers were numbered from the base to the smallest step. Layers 1 and 75 were taken as the endpoints of a line that was drawn to mark where the layers should reside. This was set as the datum in the x-direction of the measurement machine. According to the set axis, the furthest point to the left of each layer was taken to monitor the distance between that layer, and the reference line made by the first and last layers. The values were recorded and a graph was made to compare the tolerances allowed by the unmodified printer, and whether it was comparable to the current modified 3D printer.

The compiled data gave fluctuating values for both FDM1 and FDM2. As can be seen in Figure 5.14., the tolerance for both systems are well within +51µm (0.0020") and -25µm (0.0010"). These results conclude that in the current state of FDM2 with the modified leveling plate and the portable build platform, the printed parts have no more error than those created on an unmodified machine. With that conclusion validated by the data gathered, attention was focused on inserting the pauses in-between specified points of the build.

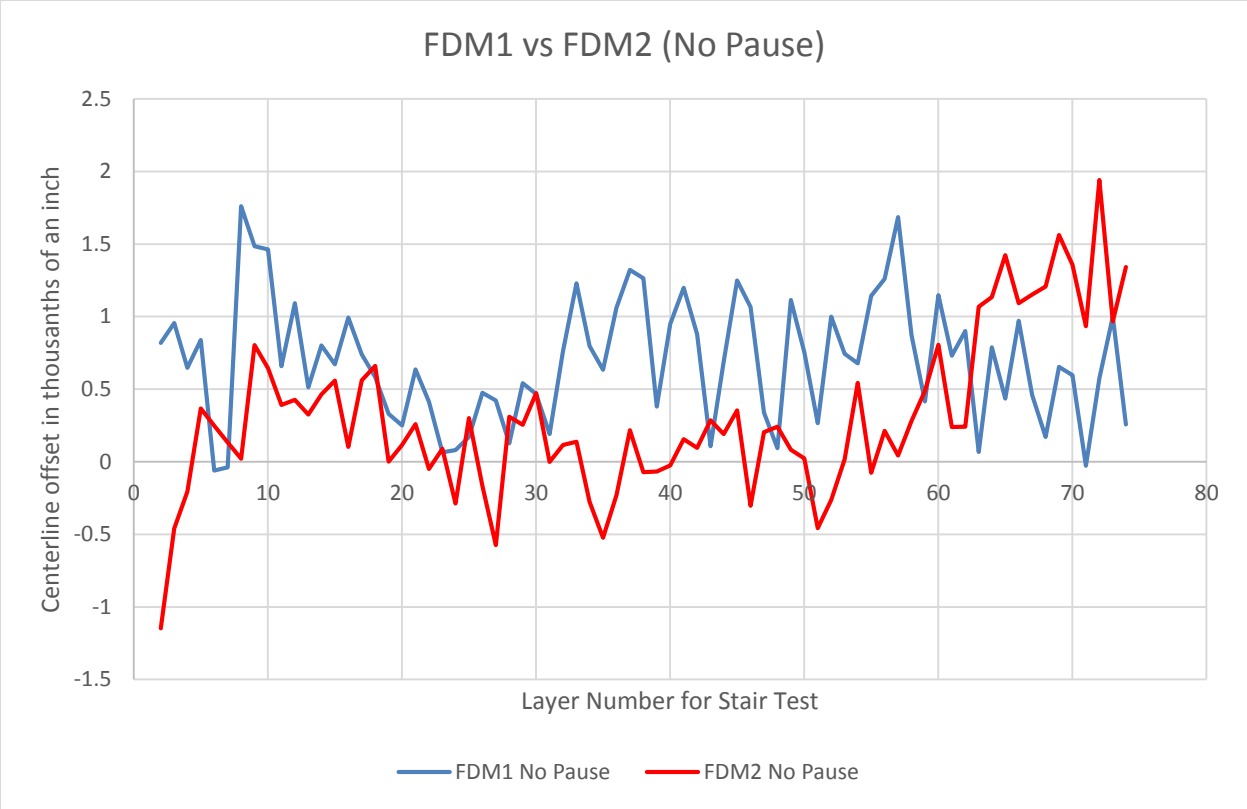

Figure 5.14. Graph of centerline layer offsets between FDM machines (No Pause)

Pausing during the build of the step, will allow for the study of the inaccuracy of the machine itself, in comparison to the method of the Multi^{3D} System, which involves the complete removal of the build platform. A pause can be inserted in a build so that the printer will stop, and allow access to the user. Four pauses were strategically positioned in the print to identify offsets easily. The pauses were made two layers before the end of the first two steps, and one layer after the start of the proceeding step. In other words, pauses were made after the twenty-third layer, the twenty-sixth layer, the forty-eighth layer, and the fifty-first layer. For FDM1 (unmodified machine), at the time of each of the four pauses, the method that was executed was very simple. The user would resume the build without opening the door or making any other changes. The printer would then resume by printing the next layer directly onto the last one deposited. For FDM2, the process involved a more complex method. At each of the pauses that were made by the printer, the VI's were implemented to complete the following motions by the robot. First, the envelope was lifted from the table where it rests, and placed inside FDM2 over the platform. Next,

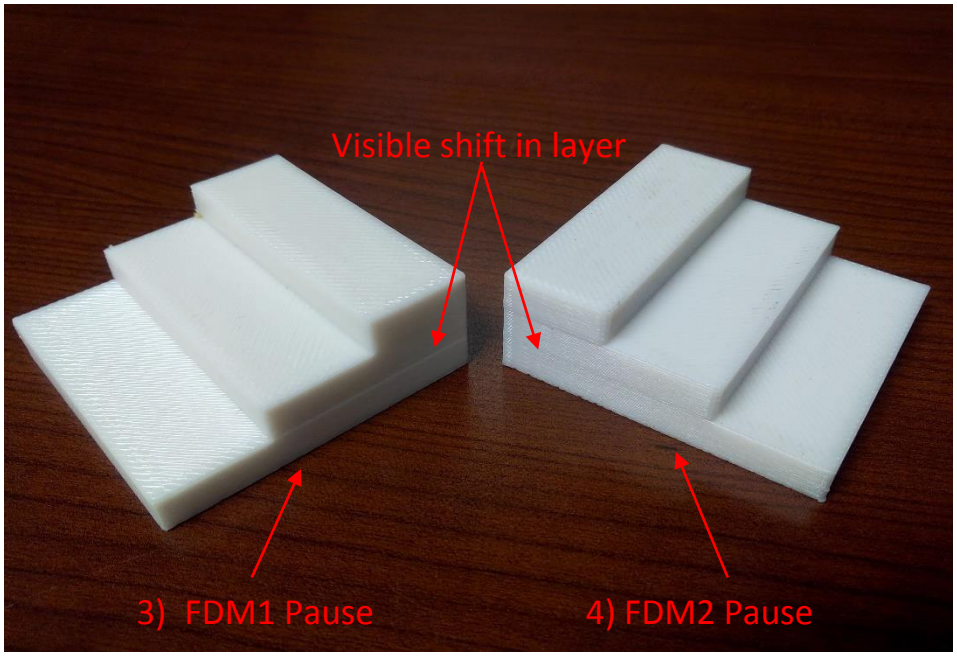

Figure 5.15. The printed steps with pauses, FDM1 (Unmodified) and FDM2 (Modified)

the entire assembly was removed from FDM2 to a position where the FDM machine's door could close. Then, the platform and envelope were placed inside the FDM machine, and the traveling envelope was removed and returned to the table it rested on when not in use. The job was then resumed and the printer continued with the next layer. It is expected that there will be inaccuracies in the FDM2 stair because the robot completely removes the job being printed, and has to place it in the same position to continue the print. The steps noticeably divided by the layers in which the pauses were inserted, meaning that in both 3D printers, no exact transition after pausing was possible. Figure 5.15., provides a visual representation of the second set of stairs utilizing pauses. Once again, there does not appear to be a differentiation between the two specimens visually. However, the measurement machine allowed a closer look into what the offset values of the layers were, and what the tolerance of each machine was.

The graph that is shown on Figure 5.16., shows the variation of the layers based on the reference line. Considering the difference between the two printers, the data shows that there is a tolerance of +0.002" and -0.001" for the unmodified FDM machine (FDM1), while the modified machine has a tolerance of +0.002"/-0.002". In terms of percent error, there was a 33% increase

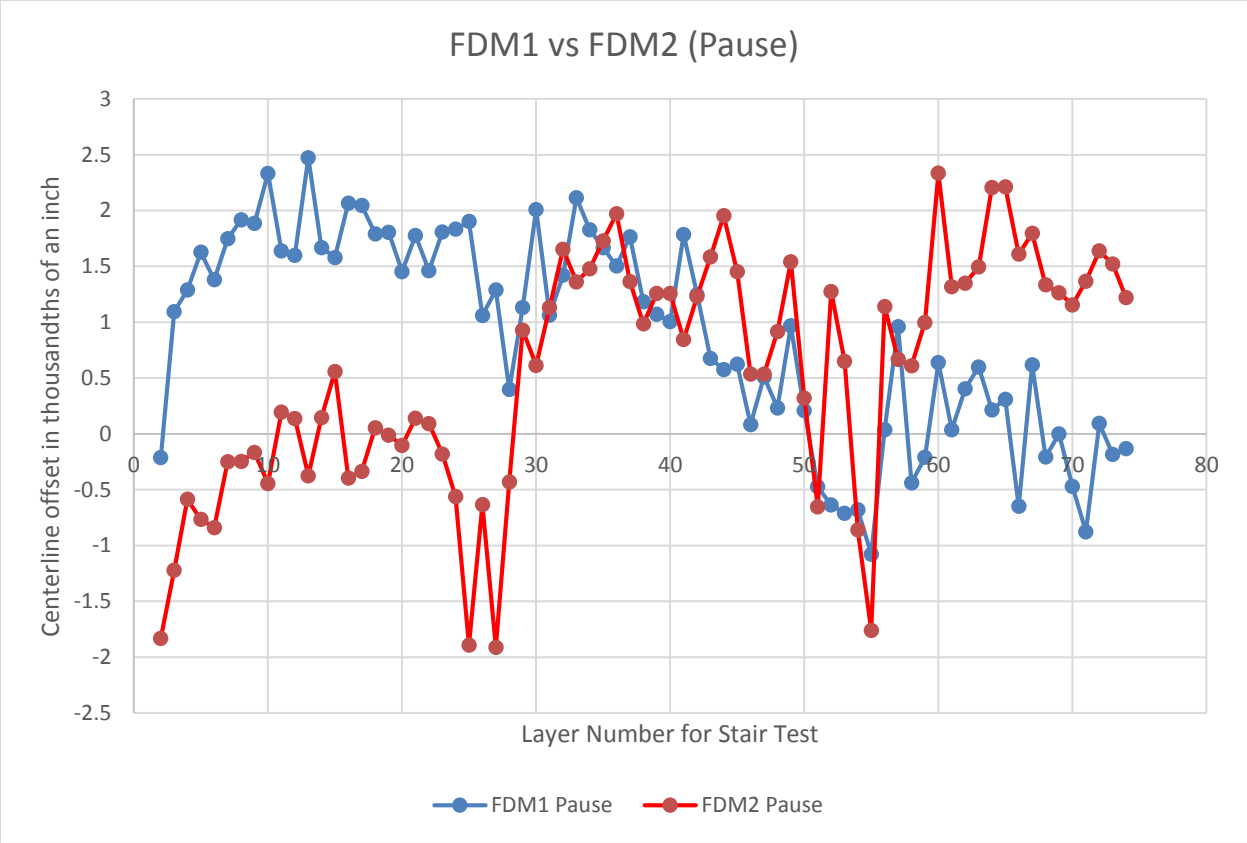

Figure 5.16. Graph of centerline layer offset between FDM (Pause)

in range of layer position relative to a datum line when the portable platform was moved after four pause operations. Although a degree of error was expected from FDM2, it was not to a greater extent to that of the unmodified FDM1. Overall, compared to the prints without the pauses, there were changes in both the machines in the tolerance of layer displacement. Neither was much more than the other, with results in the thousandths of an inch.

Conclusions gathered from this experiment strengthen the implementation of the portable build platform as a method of transferring parts within the Multi^{3D} System, while avoiding large registration error and misalignments. The offsets encountered within the modified FDM2 machine were noteworthy, however, when compared to results from the original manufacturers version of the printers, it is determined that there is no major change in the range of offsets. Efforts will be made to begin the modifications on the FDM1 so that the platform will have another manufacturing

station to be placed into. This will result in tests that can be completed in multiple 3D printers, including the experimentation in the multi-material part fabrication.

CHAPTER 6

Discussion

6.1 Conclusion

After several tests were conducted with the Multi^{3D} System, it was possible to extract conclusions from the data. The matrix calculations of the robot, along with the 3D plots of motion, served their purpose in the simulation of the arrangement of manufacturing stations. Considering no stations were present at the time of the simulations, it is possible to confirm that they were a good measure by which to construct the system. Results showed no problems in the retraction of the robot, and successful collision avoidance. The Mock FDM machines provided excellent practice props, which allowed for the establishment of the robot movement methodology. Once complete, the motions of the robot were successfully transferred to the actual FDM machines.

Other positive conclusions were found in the stair step test. Results in chapter 5 help to verify that although previously thought that the placing and removing of the platform would cause a rise in inaccuracies, as well as have warped printed parts, that was not the case. There was promising data collection, as the offset found in the results of the pause test affirmed that there was not much offset in the modified 3D printer comparted to an unmodified factory setting 3D printer. Validation of the printers and the system as a whole, shift the focus on the future work of the Multi3D system and the recommendations to continuing this work.

6.2 Recommendations

In order to improve upon the research conducted on the Multi^{3D} System, it is recommended that more testing be done on the varying parameters of the parts being build. This can range from printing different sized parts, to printing with multiple materials. Future work on

the Multi^{3D} System would include the insertion of cavities into the printed parts with the CNC router, placing electronic components into the cavities, then printing over them. This would produce the final product desired for the project, a multi-functional 3D printed part.

Other recommendations include the manufacturing of a second build platform to explore parallel manufacturing. Printing two parts at once, then interacting with the CNC, would give maximum validation to the use of the robot arm in handling complex placement. A final recommendation given would be to incorporate more manufacturing stations, in addition to the two FDM printers and the CNC router. A wire embedding station is suggested, as well as the use of the computer vision station for part quality control. Any of these recommendations would bring about results that have not been explored by other promoters of AM.

References

Berman, B. (2012). 3-D printing: The new industrial revolution. *Business Horizons, 55*, 155-162.

Brogårdh, T. (2007). Present and future robot control development-An industrial perspective. *Annual Reviews in Control, 31*(1), 69-79.

Denavit, J., & Hartenberg, R. (1955). A Kinematic Notation for Lower-Pair Mechanisms Based on Matrices. *Journal of Applied Mechanics, 22*, 215-221.

Doren, M. V., & Slocum, A. (1995). Design and Implementation of a Precision Material Handling Robot Control System. *International Journal of Machine Tools and Manufacturing, 35*(7), 1003-1014.

Espalin, D., Ramirez, J., Medina, F., & Wicker, R. (2012). Multi-Material, Multi-Technology FDM System. *Solid Freeform Fabrication Conference.*

Gibson, I., Rosen, D., & Stucker, B. (2010). *Additive Manufacturing Technologies Rapid Prototyping to Direct Digital Manufacturing.* New York: Springer.

Lewis, F. (2004). *Robot Manipulator Control Theory and Practice.* New York: Marcel Deckker.

Mavroidis, C., DeLaurentis, K., Won, J., & Alam, M. (2000). Fabrication of Non-Assembly Mechanisms and Robotic Systems Using Rapid Prototyping. *Journal of Mechanical Design, 123*(4), 516-524.

Mellor, S., Hao, L., & Zhang, D. (2014). Additive manufacturing: A framework for implementation. *Int. J. Production Economics, 149*, 194-201.

Motoman. (2011, June). *DX100 Robot Controller*. (Yaskawa Motoman Robotics) Retrieved January 2014, from http://www.motoman.com/datasheets/dx100%20controller.pdf

Motoman. (2012, January). *Yaskawa Motoman Robotics.* Retrieved January 2014, from https://www.motoman.com/datasheets/mh50_mh50-35.pdf

Ravi, J., Murugesh, B., Srivatsa, S., Sastry, P., & Raman, P. (1988). Robotic Operating System for Material Handling Robot. *Robotics and Autonomous Systems, 4*(2), 157-168.

Sayler, S., & Dillman, R. (2011). Experience-based optimization of universal manipulation strategies for industrial assembly tasks. *Robotics and Autonomous Systems, 59*(11), 882-898.

Sayler, S., & Dillmann, R. (2011). Experience-based optimization of universal manipulation strategies for industrial assembly tasks. *Robotics and Autonomous Systems, 59*, 882-898.

Spathopoulos, M., & de Ridder, M. (1999). Modelling and distributive control design of a flexible manufacturing system. *Computers in Industry, 38*(2), 155-130.

Sun, Q., Rizvi, G., Bellehumeur, C., & Gu, P. (2008). Effect of processing conditions on the bonding quality of FDM polymer filaments. *Rapid Prototyping Journal, 14*(2), 72-80.

Appendix A

MATLAB Code for Calculating T-matrices

```
% Position of the MH50 in relation to the Base
clc
clear
%Angles Input
ang1= 0;
ang2= 0;
ang3= 0;
ang4= 0;
ang5= 0;
ang6= 0;

%Lengths of Links
a1= 7.82674;
a2= 34.2520;
a3= 15.1184;
a4= 1.4567;
a5= -6.4370;
a6= 0;

%Transformation of Angles from Degrees to Radians
th0=(ang1*(pi/180));
th1=(ang1-43.1652)*(pi/180);
th2 = (ang2-90)*(pi/180);
th3=(ang3+56.848)*(pi/180);
th3o=(ang3*(pi/180));
th4=((ang4-90)*(pi/180));
th4o=(ang4*(pi/180));
th5=((ang5-90)*(pi/180));
th5o=((ang5)*(pi/180));
th6=(ang6*(pi/180));


%Calculation of the First A matrix
A1=[cos(th0)    0      -sin(th0)    a1*cos(th1);...
    sin(th0)    0       cos(th0)    a1*sin(th1);...
    0          -1         0          8.9764;...
    0           0         0              1];

%Calculation of Second A matrix
A2=[cos(th2)  -sin(th2)  0         a2*cos(th2);...
    sin(th2)   cos(th2)  0         a2*sin(th2);...
    0           0        1         -0.2756;...
    0           0        0             1];

%Calculation of Third A matrix
A3=[cos(th3o)    0     -sin(th3o)    a3*cos(th3);...
    sin(th3o)    0      cos(th3o)    a3*sin(th3);...
    0           -1        0          5.6299;...
```

```
    0           0        0             1];

%Calculation of the Fourth A matrix
A4=[cos(th4o)    0      sin(th4o)    a4*cos(th4);...
    sin(th4o)    0     -cos(th4o)    a4*sin(th4);...
    0           1        0           27.6969;...
    0           0        0             1];

%Calculation of the Fifth A matrix
A5=[cos(th5o)    0     -sin(th5o)    a5*cos(th5);...
    sin(th5o)    0      cos(th5o)    a5*sin(th5);...
    0          -1        0           -1.2992;...
    0           0        0             1];

%Calculation of the Sixth A matrix
A6=[cos(th6)  -sin(th6)  0         a6*cos(th6);...
    sin(th6)   cos(th6)  0         a6*sin(th6);...
    0           0        1         0.4528;...
    0           0        0             1];


%Calculation of Each individual T matrix
%Link 1
T1=A1;
%Link 2
T2=A1*A2;
%Link 3
T3=A1*A2*A3;
%Link 4
T4=A1*A2*A3*A4;
%Link 5
T5=A1*A2*A3*A4*A5;
%Link 6
T6=A1*A2*A3*A4*A5*A6
```

Semicolon used to suppress the output of the data.
Can be removed to find the position of selected link
in relation to the base.

Appendix Table 1.1. Pulses stored for the use of the robot

Position #	Pulses for each of the six axes					
Platform to FDM2	S	L	U	R	B	T
7	253781	-1071	-111646	488	41833	1449
8	254004	41167	-46791	368	37098	1473
9	254005	41034	-46753	368	37021	1474
10	254004	39286	-46190	370	35975	1470
11	253988	11124	-91255	353	39826	1493
12	253693	-39850	-144274	602	35857	1374
Envelope to Table						
18	200880	-46622	-151306	-21448	38119	10376
19	185057	31004	-63753	-9455	39440	5288
20	185057	30843	-63700	-9479	39440	5288
21	185218	28255	-62724	-9879	37796	5617
22	195403	-28350	-132592	-17124	38692	8557
Envelope to FDM2						
29	253381	-27845	-101556	1644	25251	722
30	253787	29768	-29270	1244	24992	920
31	253787	29690	-29158	1248	24911	918
32	253844	27989	-26615	1265	23122	993
33	253869	-4085	-71061	1168	24868	1058
34	253523	-55693	-117606	2037	18120	529

Appendix Table 1.2. Laser displacement sensor data for platform

Measurement Number	Top-Left (with bars)	Top-Left (without bars)	Back (with bars)	Back (without bars)
1	-2482.5 µm	-1555.0 µm	4230.0 µm	5095.0 µm
2	-2593.0 µm	-1540.0 µm	3855.5 µm	4619.5 µm
3	-2455.5 µm	-1484.5 µm	3148.0 µm	4182.0 µm
4	-2375.5 µm	-1528.5 µm	3254.5 µm	4050.0 µm
5	-2391.5 µm	-1642.5 µm	3223.0 µm	3965.0 µm
6	-2510.0 µm	-1737.5 µm	3203.0 µm	3984.0 µm
7	-2422.5 µm	-1952.5 µm	3191.0 µm	3906.0 µm
8	-2313.5 µm	-1856.5 µm	3036.0 µm	3902.5 µm
9	-2115.5 µm	-1861.0 µm	3244.0 µm	3800.0 µm
10	-2598.5 µm	-1893.0 µm	3243.0 µm	3850.5 µm
STDEV	142.04 µm	175.86 µm	374.54 µm	410.57 µm

Appendix Table 1.3. Laser displacement sensor data for envelope

Measurement Number	Distance between Envelope and Laser sensor
1	-237.5 µm
2	-237.5 µm
3	-237.5 µm
4	-237.5 µm
5	-700.5 µm
6	-710.0 µm
7	-1310.5 µm
8	-238.5 µm
9	-238.5 µm
10	-237.5 µm

Vita

Jose Luis Coronel Jr. was born on March 18, 1992 and is the son of Mrs. Evangelina Lugo Coronel and Mr. Jose Luis Coronel. Jose received his high school diploma in May of 2009 from Canutillo High School, where he held the honor of being valedictorian. He obtained a Bachelor of Science Degree in Mechanical Engineering with *summa cum laude* distinction from the University of Texas at El Paso in May of 2013. As an undergraduate, Jose was a member of the National Society of Collegiate Scholars where he served as Vice-President for Community Service. He frequently tutored high school students throughout his time at UTEP, as well as advised them as they became students of the university.

Permanent address: 898 Vinton Avenue
Canutillo, TX, 79835

This thesis was typed by Jose Luis Coronel Jr.